Thermodynamics of regular black holes in anti-de Sitter space

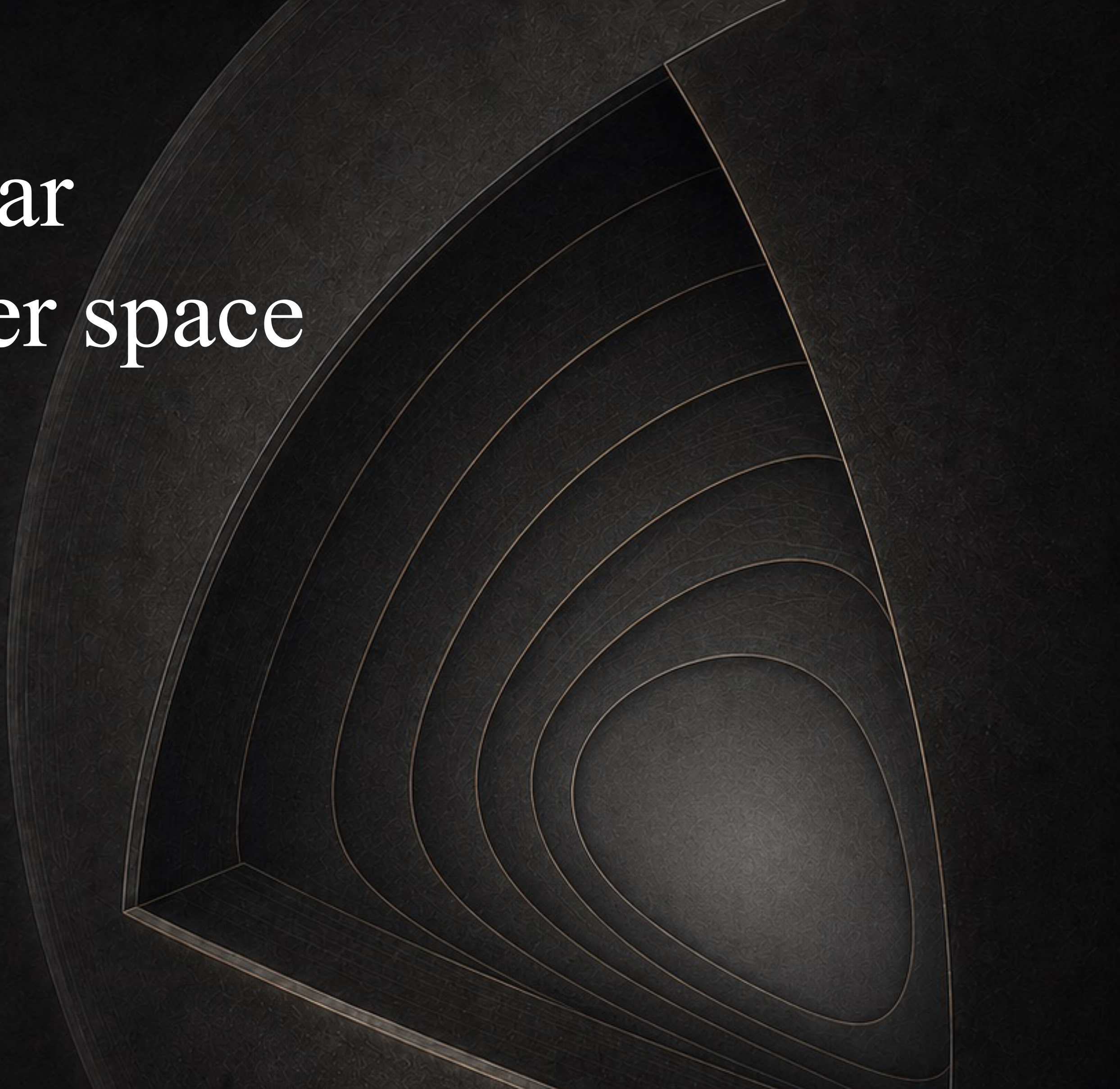

Sebastian Murk

Faculty of Mathematics and Physics
Charles University

Thermality in Quantum Field Theory in Curved Spacetimes
Principia Institute, São Paulo, Brazil
6 August 2026

Paper + Collaborators

Thermodynamics of Regular Black Holes in Anti-de Sitter Space

Robie A. Hennigar,[a] **David Kubizňák**,[b] **Sebastian Murk**,[c] **Ioannis Soranidis**[d]

[a] *Centre for Particle Theory, Department of Mathematical Sciences, Durham University, Durham DH1 3LE, UK*

[b] *Institute of Theoretical Physics, Faculty of Mathematics and Physics, Charles University, V Holešovičkách 2, 180 00 Prague 8, Czech Republic*

[c] *Quantum Gravity Unit, Okinawa Institute of Science and Technology, 1919-1 Tancha, Onna-son, Okinawa 904-0495, Japan*

[d] *School of Mathematical and Physical Sciences, Macquarie University, Sydney, New South Wales 2109, Australia*

JHEP **2025** (11), 121

arXiv:2505.11623 [gr-qc]

Robie A. Hennigar

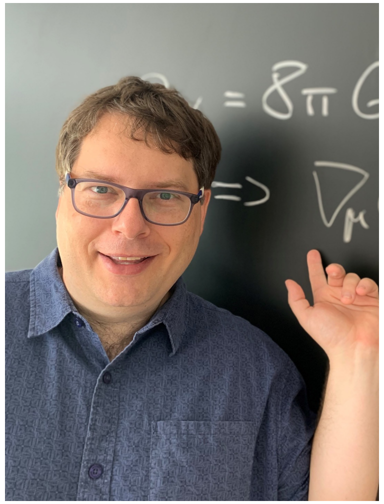

David Kubizňák

Ioannis Soranidis

Durham University

Faculty of Mathematics and Physics
Charles University

MACQUARIE University
SYDNEY · AUSTRALIA

OIST OKINAWA INSTITUTE OF SCIENCE AND TECHNOLOGY

Background and context

Are the singularities of GR resolved in nature? And if so, how?

Singularity-free BH metrics: *Bardeen*[1968]*, Dymnikova*[1992]*, Hayward*[2006]*, etc.*

Note: these metrics are not *a priori* solutions of any known theory. ➡ **kinematics** (rather than dynamics)

Note: realizing RBHs as exact solutions of any realistic theory is difficult.

Recent progress: Schwarzschild singularity is resolved generically in $D \geq 5$ when an infinite tower of higher-order curvature corrections is added to EH action.

Bueno, Cano, Hennigar
Phys. Lett. B **861**, 139260 (2025)

- Singularity is resolved without any additional fields
- Second-order field equations in spherical symmetry
- Birkhoff theorem: static solution is the unique one

Bueno, Cano, Hennigar, Murcia
Phys. Rev. Lett. **134**, 181401 (2025)

➡ **RBH dynamics**

Paper + Collaborators

Thermodynamics of Regular Black Holes in Anti-de Sitter Space

Robie A. Hennigar,[a] **David Kubizňák**,[b] **Sebastian Murk**,[c] **Ioannis Soranidis**[d]

[a] *Centre for Particle Theory, Department of Mathematical Sciences, Durham University, Durham DH1 3LE, UK*

[b] *Institute of Theoretical Physics, Faculty of Mathematics and Physics, Charles University, V Holešovičkách 2, 180 00 Prague 8, Czech Republic*

[c] *Quantum Gravity Unit, Okinawa Institute of Science and Technology, 1919-1 Tancha, Onna-son, Okinawa 904-0495, Japan*

[d] *School of Mathematical and Physical Sciences, Macquarie University, Sydney, New South Wales 2109, Australia*

JHEP **2025** (11), 121

arXiv:2505.11623 [gr-qc]

Our JHEP paper extends this framework by

1. Considering a cosmological constant
2. Constructing asymptotically AdS black holes
3. Including minimally coupled matter
4. Analyzing thermodynamic properties

Durham University

Faculty of Mathematics and Physics
Charles University

MACQUARIE University
SYDNEY · AUSTRALIA

OIST OKINAWA INSTITUTE OF SCIENCE AND TECHNOLOGY

RBHs in quasitopological gravity

EoM of gravity theory with Lagrangian density $\mathcal{L}(g^{ab}, R_{abcd})$ and minimally coupled matter:

$$\mathcal{E}_{ab} \equiv P_a^{\ cde} R_{bcde} - \tfrac{1}{2} g_{ab} \mathcal{L} - 2\nabla^c \nabla^d P_{acdb} = 8\pi G_{\mathrm{N}} T_{ab}$$

$\boxed{\textbf{Quasitopological gravity:} \quad \nabla^d P_{acdb} = 0}$

for spherical, planar, or hyperbolic symmetry

$\Longrightarrow$ second-order EoM

Can be constructed via a recurrence relation:

$$\mathcal{Z}_{n+5} = -\frac{3(n+3)}{2(n+1)D(D-1)} \mathcal{Z}_1 \mathcal{Z}_{n+4} + \frac{3(n+4)}{2nD(D-1)} \mathcal{Z}_2 \mathcal{Z}_{n+3} - \frac{(n+3)(n+4)}{2n(n+1)D(D-1)} \mathcal{Z}_3 \mathcal{Z}_{n+2} .$$

Action: $\quad I = I_{\mathrm{QT}} + I_{\mathrm{matter}} \, , \quad I_{\mathrm{QT}} = \int \frac{\mathrm{d}^D x \sqrt{|g|}}{16\pi G_{\mathrm{N}}} \left[-2\Lambda + R + \sum_{n=2}^{\infty} \tilde{\alpha}_n \mathcal{Z}_n \right]$

Variation: $\quad \mathcal{E}_{ab} = 8\pi G_{\mathrm{N}} T_{ab}$ with $\mathcal{E}_{ab} = \frac{16\pi G_{\mathrm{N}}}{\sqrt{|g|}} \frac{\delta I_{\mathrm{QT}}}{\delta g^{ab}}$ and $T_{ab} = -\frac{2}{\sqrt{|g|}} \frac{\delta I_{\mathrm{matter}}}{\delta g^{ab}}$

RBHs in quasitopological gravity

General static metric with maximally symmetric transverse sections:

$$\begin{aligned} k = +1 &: \quad \text{spherical} \\ k = 0 &: \quad \text{planar} \\ k = -1 &: \quad \text{hyperbolic} \end{aligned}$$

$$ds^2 = -N(r)^2 f(r) dt^2 + \frac{dr^2}{f(r)} + r^2 \Omega_{ij}\, dx^i\, dx^j,$$

where Ω_{ij} is the metric on a (D-2)-dimensional space with curvature tensor $R_{ijkl} = k\left(\Omega_{ik}\Omega_{jl} - \Omega_{il}\Omega_{jk}\right)$.

Assume minimally coupled matter inherits the symmetry of the spacetime: $T_t^t = T_r^r \Rightarrow N'(r) = 0 \implies N = 1$

The natural radial curvature variable is $\psi(r) \equiv \dfrac{k - f(r)}{r^2}$.

The gravitational theory is encoded by the function $h(\psi) \equiv -\dfrac{2\Lambda}{(D-1)(D-2)} + h_f(\psi),$

where $\quad h_f(\psi) \equiv \psi + \displaystyle\sum_{n=2}^{\infty} \alpha_n \psi^n, \quad \alpha_n \equiv \frac{D-2n}{D-2}\tilde{\alpha}_n.$

Integrated radial field equation:

$$\underbrace{h_f\big(\psi(r)\big)}_{\substack{\text{gravitational couplings} \\ +\ \text{metric } f(r)}} = \underbrace{\mathcal{S}(r)}_{\substack{\text{cosmological constant} \\ +\ \text{mass} + \text{matter}}}$$

$$\boxed{\psi(r) = h_f^{-1}\big(\mathcal{S}(r)\big) \implies f(r) = k - r^2 h_f^{-1}\big(\mathcal{S}(r)\big)}$$

RBHs in quasitopological gravity

Integrated radial field equation:

$$\underbrace{h_f\big(\psi(r)\big)}_{\substack{\text{gravitational couplings}\\ +\text{ metric } f(r)}} = \underbrace{\mathcal{S}(r)}_{\substack{\text{cosmological constant}\\ +\text{ mass }+\text{ matter}}}$$

$$\boxed{\psi(r) = h_f^{-1}\big(\mathcal{S}(r)\big) \implies f(r) = k - r^2 h_f^{-1}\big(\mathcal{S}(r)\big)}$$

Asymptotically flat vacuum: $\mathcal{S}(r) = \frac{m}{r^{D-1}}$,

Asymptotically AdS vacuum: $\mathcal{S}(r) = -\frac{1}{L^2} + \frac{m}{r^{D-1}}$,

Asymptotically AdS with matter: $\mathcal{S}(r) = -\frac{1}{L^2} + \frac{m}{r^{D-1}} + \mathcal{S}_{\text{matter}}(r)$.

where $\mathcal{S}_{\text{matter}}(r) \equiv -\frac{16\pi G_{\text{N}}}{(D-2)r^{D-1}} \int_\infty^r \tilde{r}^{\,D-2} T^t{}_t(\tilde{r})\, d\tilde{r}$

Keep in mind:

1. The solutions are exact solutions of specified field equations, not phenomenological metrics.
2. Quasitopological densities exist at all curvature orders in $D \geq 5$, enabling the infinite resummation required for regularity.
3. The action makes quantities such as Wald entropy, conserved mass, the first law, and (in principle) gravitational dynamics well-defined.

Horizon structure of spherical AdS solutions ($\Lambda < 0, k = +1$)

$$\Lambda = -\frac{(D-1)(D-2)}{2L^2}, \quad \mathcal{S}(r) = -\frac{1}{L^2} + \frac{m}{r^{D-1}}.$$

Consider Hayward-AdS metric as a representative example:

$$f(r) = 1 - \frac{r^2 \mathcal{S}(r)}{1 + \alpha \mathcal{S}(r)}.$$

At large r, the solution approaches AdS with

$$L_{\text{eff}}^2 = L^2 - \alpha, \quad a \equiv \frac{\alpha}{L^2}, \quad \frac{G_{\text{eff}}}{G_{\text{N}}} = \frac{L^4}{L_{\text{eff}}^4} = \frac{1}{(1-a)^2}.$$

The ADM/thermodynamic mass is given by

$$M = \frac{(D-2)\Omega_{D-2}}{16\pi G_{\text{N}}} m.$$

integration constant

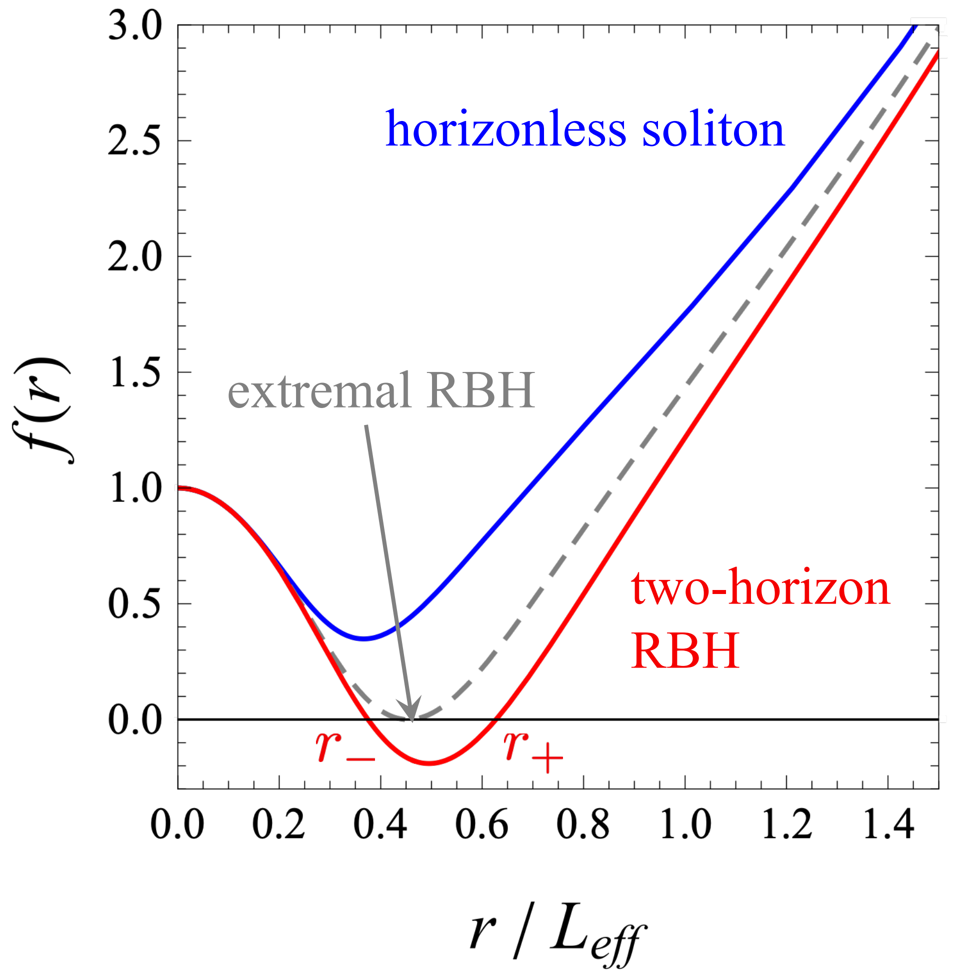

$$k = 1, \quad D = 5, \quad a = 0.1, \quad L_{\text{eff}} = G_{\text{eff}} = 1,$$

$$[M_{\text{blue}}, M_{\text{gray}}, M_{\text{red}}] = [0.3, 0.706, 1].$$

Regular Maxwell-charged solutions

For the Maxwell theory: $\mathcal{S}_{\text{EM}}(r) = -\frac{1}{L^2} + \frac{m}{r^{D-1}} - \frac{q^2}{r^{2(D-2)}}$.

$r \to \infty$

At large r, the charge is subleading, so L_{eff} and G_{eff} derived from the asymptotic behavior of the metric are the same as before. **However, the charge-dependent contribution to $\mathcal{S}(r)$ dominates at small r.**

➡ **Regular Maxwell-charged configurations have AdS cores.**

$$f(r) = k + \frac{r^2}{|\alpha|} + \mathcal{O}\left(r^3\right), \quad r \to 0.$$

NB: The geometry can be regular even though the Maxwell field diverges: $|E_{\text{EM}}(r)| \propto \frac{|q|}{r^{D-2}} \xrightarrow{r\to 0} \infty$.

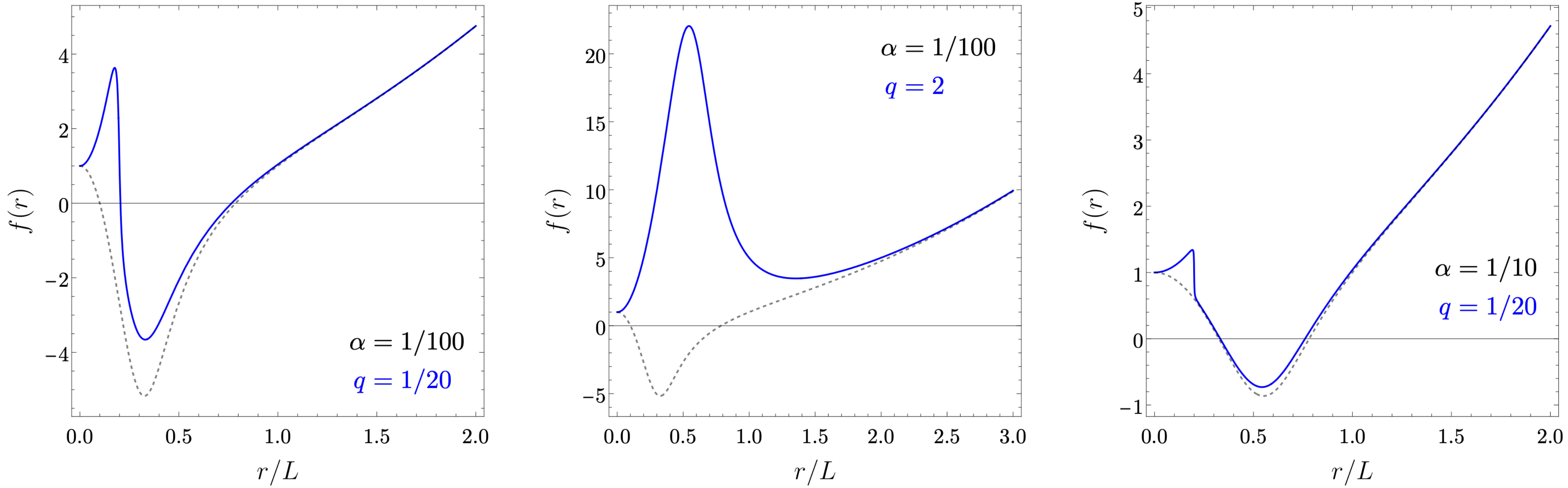

From regular metrics to fully regular charged solutions

So far: RBH (regular geometry) coupled to Maxwell electrodynamics (divergent electric field)

Now: Use nonlinear electrodynamics (NLE) to cure divergence of the electric field

NLE theory

We consider ***Born–Infeld*** and ***RegMax*** NLE theories.

$$T^{\mu\nu} = -\frac{1}{4\pi}\left(4F^{\mu\sigma}F^{\nu}{}_{\sigma}\mathcal{L}_{\mathcal{F}} - \mathcal{L}g^{\mu\nu}\right)$$

Both reduce to Maxwell electrodynamics in the weak-field regime.

$\mathcal{S}(r)$ $f(r)$

➡ Their large r asymptotics reproduce the charged Maxwell case.

But: Their small r behavior is decisively different!

Recall: $f(r) = k - \frac{r^2}{|\alpha|}\lim_{r\to 0}\mathrm{sign}(\mathcal{S}(r)) + \cdots.$

$$\mathcal{S}_{\mathrm{BI}}(r) = \frac{m - m_\star}{r^{D-1}} + \sqrt{\frac{8(D-3)}{D-2}}\,\frac{b|q|}{r^{D-2}} + \cdots, \qquad \mathcal{S}_{\mathrm{RegMax}}(r) = \frac{m - m_\star}{r^{D-1}} + \cdots,$$

where

$m_\star$: finite electrostatic self-energy

b : BI limiting field strength

$|E_{\mathrm{BI}}(0)| = b, \quad b \to \infty \Rightarrow \text{Maxwell}$

Possible outcomes:

$m > m_\star$:	dS core
$m = m_\star$:	dependent on subleading term in $\mathcal{S}(r)$
$m < m_\star$:	AdS core

Extended first law and Smarr relation

First law: $dM = T\,dS + V\,dP + \Psi\,d\alpha$

Smarr: $(D-3)M = (D-2)TS - 2VP + 2\alpha\Psi$

where $\Psi = \dfrac{1}{2\alpha}[(D-3)M - (D-2)TS + 2PV]$ is a potential conjugate to the coupling constant α.

When a Maxwell field is included: additional U(1) charge $\mathcal{Q} = \dfrac{\sqrt{2(D-2)(D-3)}}{8\pi G_{\mathrm{N}}}\Omega_{D-2}q$

First law: $dM = T\,dS + \Phi\,d\mathcal{Q} + V\,dP + \Psi\,d\alpha$

Smarr (Maxwell): $(D-3)M = (D-2)TS + (D-3)\Phi_{\mathrm{EM}}\mathcal{Q} - 2VP + 2\alpha\Psi$

In NLE theories: additional length scale associated with their coupling constants

$$(D-3)M = (D-2)TS + (D-3)\Phi_i\mathcal{Q} - 2VP + 2\alpha\Psi + [b_i]b_i\mathcal{B}_i$$

Wald entropy for Hayward-AdS model

When the horizon radius becomes comparable to the regularization length, higher-order terms with a potentially negative denominator are no longer suppressed for certain dimensions D.

For BHs sufficiently close to extremality, the Wald entropy can become negative.

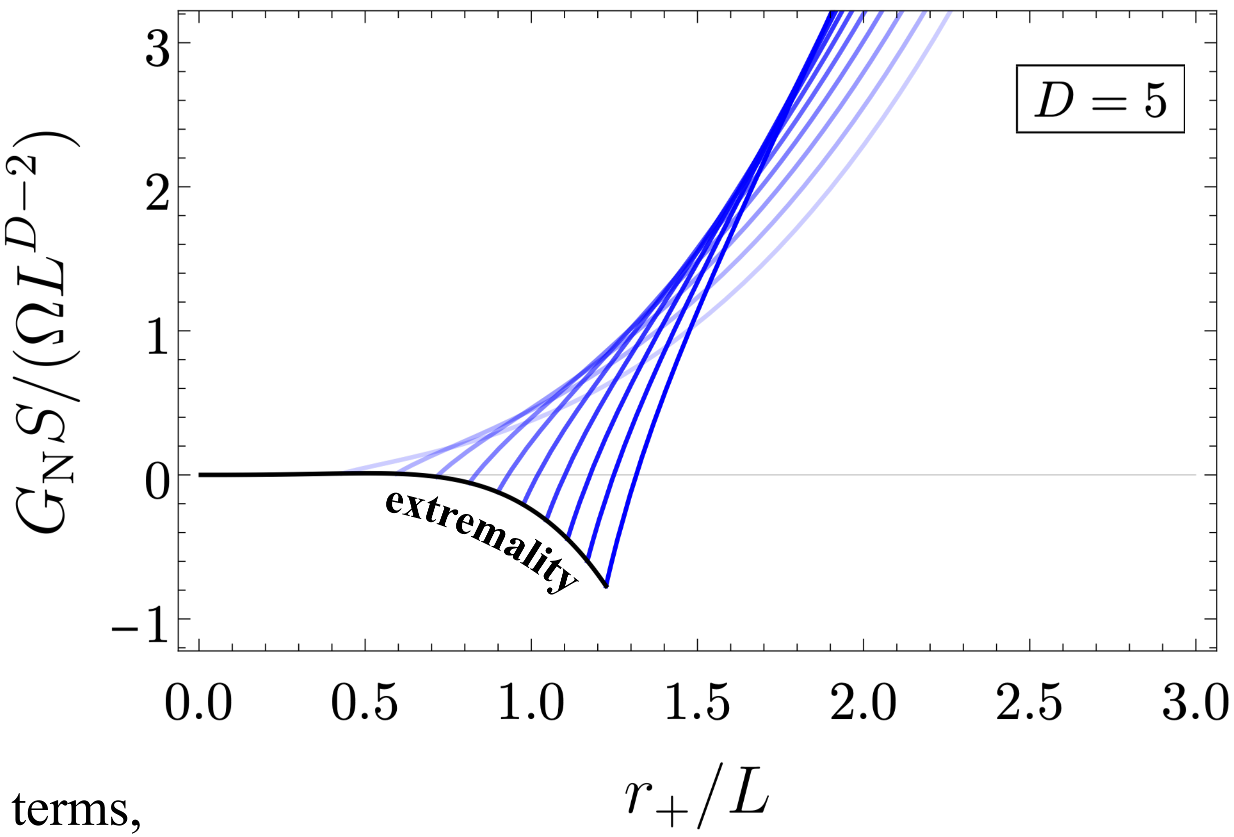

However:

1. Wald entropy is sensitive to *all* higher-curvature terms, irrespective of whether they produce dynamics or not.
   - ➡ Can always shift it by an overall constant by adding suitable derivative terms to the action.
2. Solutions with negative Wald entropy occur close to extremality at very low Hawking temperature.
   - ➡ Cannot expect that semiclassical computation of entropy will be reliable anyway.

Equation of state and P-v diagram for Hayward AdS black hole

From the definition of thermodynamic pressure,

$$P = -\frac{\Lambda}{8\pi G_N} = \frac{(D-1)(D-2)}{16\pi G_N L^2}$$

we can obtain the equation of state

$$P = \frac{(D-2)r_+^3 T}{4G_\mathrm{N}(r_+^2-\alpha)^2} - \frac{(D-2)\left[(D-3)r_+^2 - \alpha(D-1)\right]}{16\pi G_\mathrm{N}(r_+^2-\alpha)^2}$$

α plays the role of an effective molecular volume.

Critical-point conditions: $\left(\frac{\partial P}{\partial v}\right)_T = \left(\frac{\partial^2 P}{\partial v^2}\right)_T = 0$

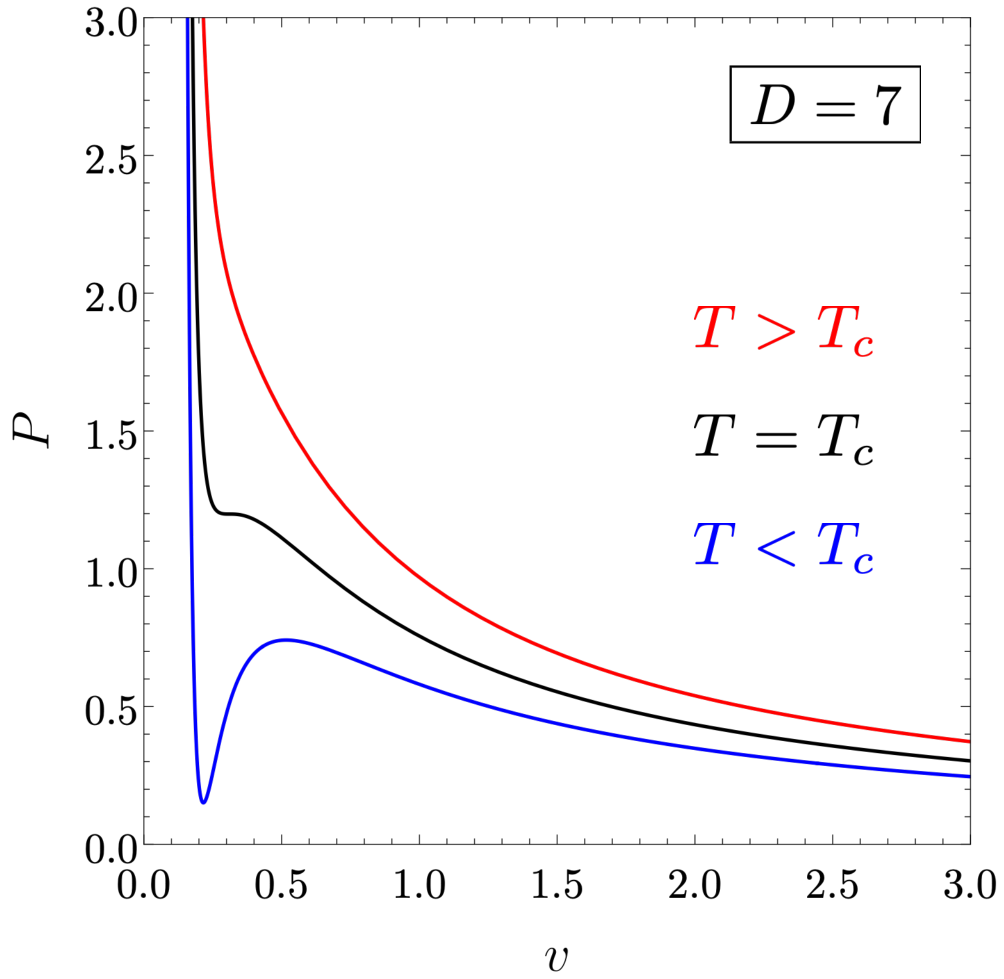

$T > T_c$: monotonic, ideal-gas-like behavior.

$T = T_c$: inflection point marking the second-order critical endpoint.

$T < T_c$: van der Waals oscillation associated with SBH/LBH coexistence.

$$v \equiv \frac{4G_N r_+}{D-2}.$$

Phase diagram for Hayward-AdS black hole

Hawking-Page transition is physical in any odd D.

At each point (T, P), the phase with the lowest free energy

$$F = M - TS$$

dominates. On a coexistence line $F_1 = F_2$.

Triple point where the three phases of thermal AdS, SBH, and LBH meet.

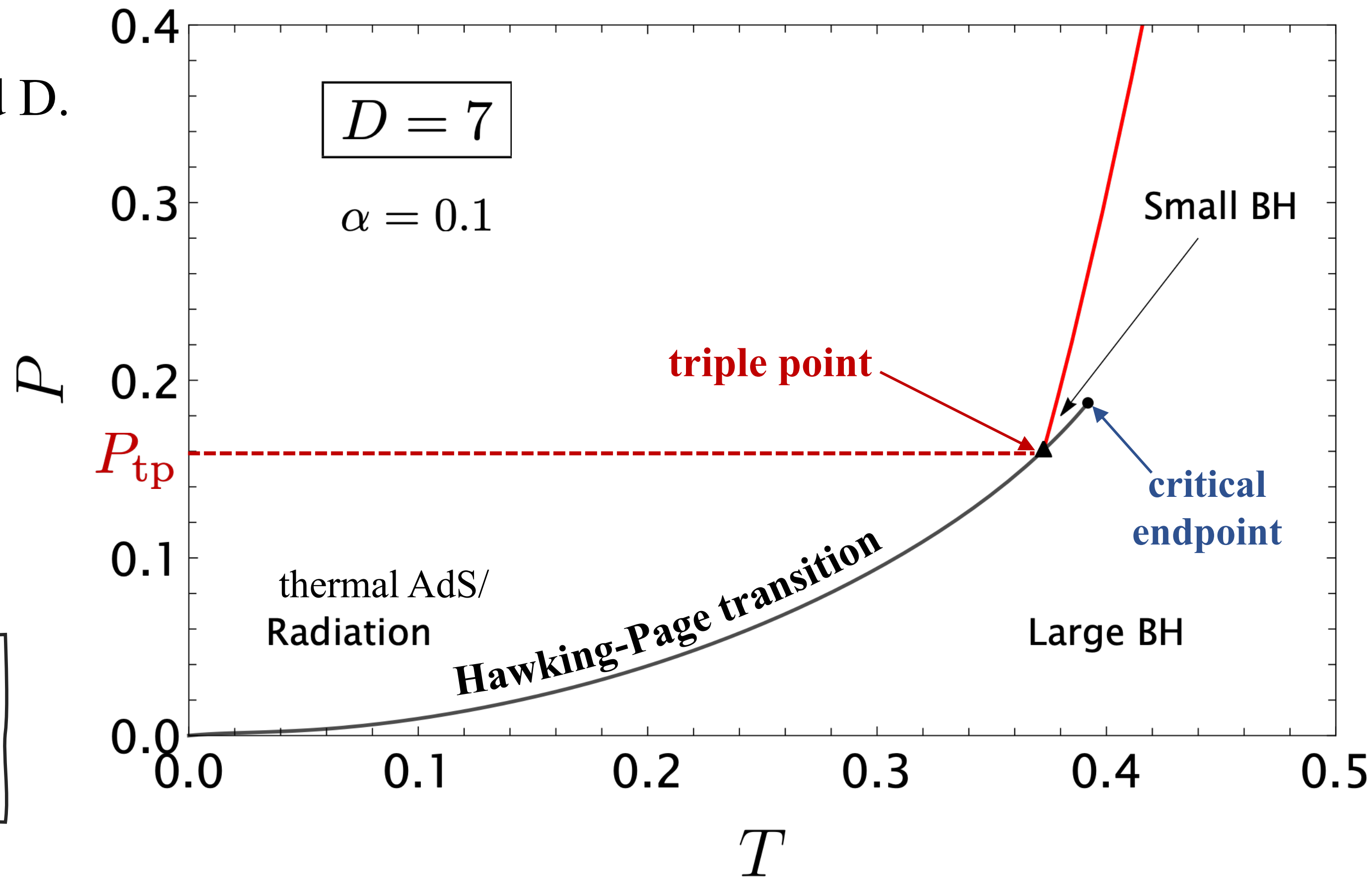

$$P < P_{\rm tp}: \quad \text{thermal AdS} \xrightarrow{\text{Hawking-Page}} \text{LBH}$$

$$P_{\rm tp} < P < P_c: \quad \text{thermal AdS} \xrightarrow{\text{Hawking-Page}} \text{SBH} \xrightarrow{\text{first-order}} \text{LBH}$$

Why a regular core makes the pressure diverge at finite volume

For spherical vacuum solutions with positive mass: $\mathcal{S}(r) \xrightarrow{r\to 0} +\infty.$

Recall: $\mathcal{S}_{\mathrm{vac}}(r) = -\dfrac{1}{L^2} + \dfrac{m}{r^{D-1}}.$

A regular core requires the curvature to remain finite: $f(r) = 1 - \psi_\star r^2 + \cdots, \quad \psi(r) \xrightarrow{r\to 0} \psi_\star < \infty.$

But the master equation says: $h_f(\psi(r)) = \mathcal{S}(r).$

$$\psi(r) = \frac{1-f(r)}{r^2} = \frac{\psi_\star r^2 + O\left(r^3\right)}{r^2} = \psi_\star + O(r)$$

Therefore, h_f must diverge while its argument remains finite: $h_f(\psi) \xrightarrow{\psi\to\psi_*} \infty.$

Now evaluate the same curvature variable at a spherical horizon: $f\left(r_+\right) = 0, \quad \psi_+ = \dfrac{1}{r_+^2}.$

As r_+ decreases, ψ_+ eventually reaches $\psi_\star$. Since the equation of state

$$P = \frac{(D-2)h_{\mathrm{f}}'\left(\psi_+\right)T}{4r_+} - \frac{(D-2)\left[(D-1)r_+^2 h_{\mathrm{f}}\left(\psi_+\right) - 2h_{\mathrm{f}}'\left(\psi_+\right)\right]}{16\pi r_+^2}$$

contains $h_f(\psi_+)$ and $h_f'(\psi_+)$, $r_+^2 \to \dfrac{1}{\psi_\star} \implies P \to \infty.$

Because $V \propto r_+^{D-1}$, this happens at a finite, nonzero volume.

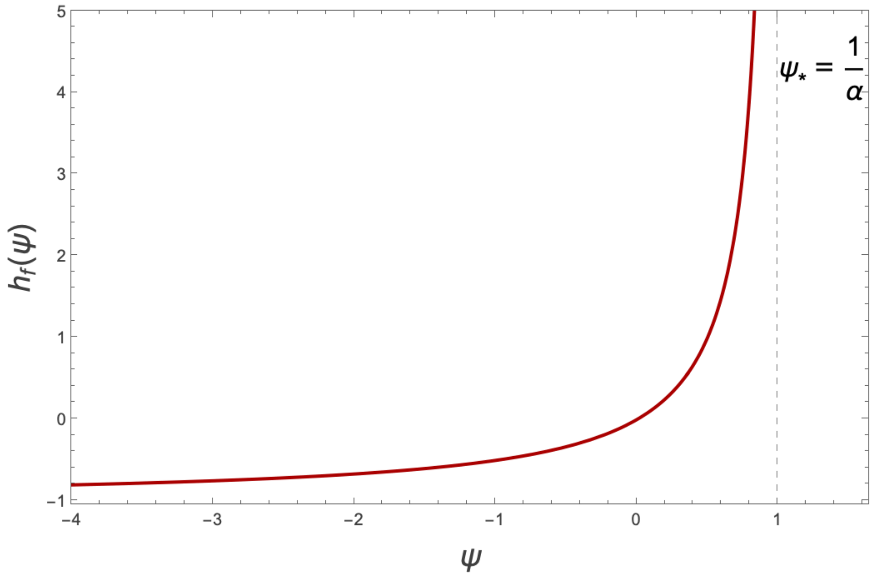

Why a regular core makes the pressure diverge at finite volume

For spherical vacuum solutions with positive mass: $\mathcal{S}(r) \xrightarrow{r\to 0} +\infty.$

Recall: $\mathcal{S}_{\text{vac}}(r) = -\dfrac{1}{L^2} + \dfrac{m}{r^{D-1}}.$

A regular core requires the curvature to remain finite: $f(r) = 1 - \psi_\star r^2 + \cdots, \quad \psi(r) \xrightarrow{r\to 0} \psi_\star < \infty.$

But the master equation says: $h_f(\psi(r)) = \mathcal{S}(r).$

$$\psi(r) = \frac{1-f(r)}{r^2} = \frac{\psi_\star r^2 + O\left(r^3\right)}{r^2} = \psi_\star + O(r)$$

Therefore, h_f must diverge while its argument remains finite: $h_f(\psi) \xrightarrow{\psi\to\psi_*} \infty.$

Now evaluate the same curvature variable at a spherical horizon: $f\left(r_+\right) = 0, \quad \psi_+ = \dfrac{1}{r_+^2}.$

As r_+ decreases, ψ_+ eventually reaches $\psi_\star$. Since the equation of state

$$P = \frac{(D-2)h_{\mathrm{f}}'\left(\psi_+\right)T}{4r_+} - \frac{(D-2)\left[(D-1)r_+^2 h_{\mathrm{f}}\left(\psi_+\right) - 2h_{\mathrm{f}}'\left(\psi_+\right)\right]}{16\pi r_+^2}$$

contains $h_f(\psi_+)$ and $h_f'(\psi_+)$, $r_+^2 \to \dfrac{1}{\psi_\star} \implies P \to \infty.$

Because $V \propto r_+^{D-1}$, this happens at a finite, nonzero volume.

For the resummations studied in our paper:

$$\psi_\star = \frac{1}{\alpha} \implies r_+^2 = \alpha.$$

Critical ratio $P_c v_c / T_c$ for various AdS models

Why do we care about this ratio?

The individual critical quantities depend on the regularization scale α,

$$v_c \propto \sqrt{\alpha}, \quad T_c \propto \frac{1}{\sqrt{\alpha}}, \quad P_c \propto \frac{1}{\alpha}$$

but their ratio does not.

$$\boxed{\Longrightarrow \quad \frac{P_c v_c}{T_c} \text{ is independent of } \alpha}$$

Differences between the curves therefore reflect the choice of resummation and the spacetime dimension, not the chosen regularization scale.

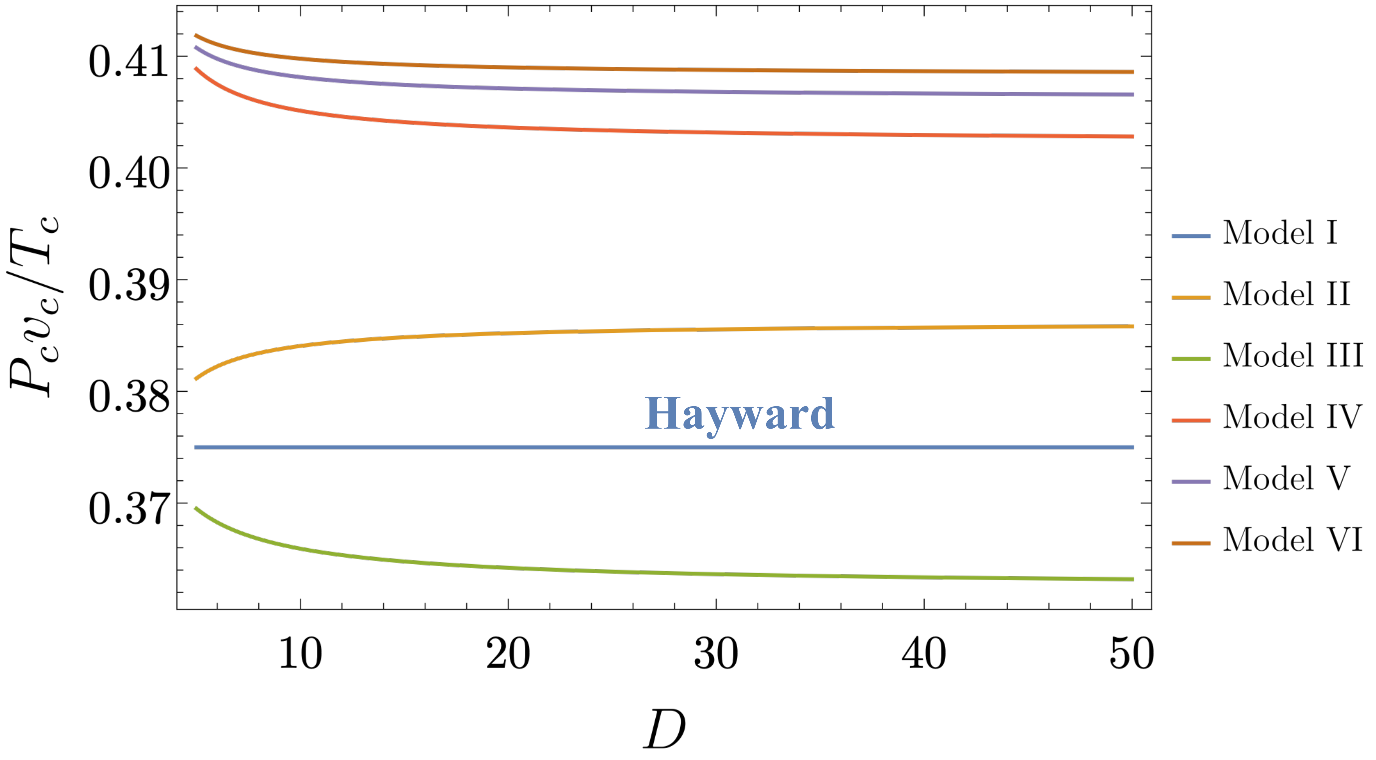

For the **Hayward-AdS model**, the ratio precisely matches the van der Waals gas in any allowed odd dimension:

$$\boxed{\frac{P_c v_c}{T_c} = \frac{3}{8}}$$

Conjectured bound for spherical vacuum RBH: $$\frac{P_c v_c}{T_c} \leq \frac{1}{2}$$

Summary of main results

1. **Quasitopological resummations yield exact regular AdS black holes in D ≥ 5.**
2. **NLE gives fully regular charged solutions; $m/m_\star$ fixes the core type.**
3. **Spherical regularity forces a finite-volume pole in the equation of state.**
4. **Hayward universally coincides with the van der Waals ratio $P_c v_c/T_c = 3/8$;**
   Surveyed models suggest an upper bound of $P_c v_c/T_c \leq 1/2$.

JHEP **2025** (11), 121

arXiv:2505.11623 [gr-qc]

Thermodynamics of Regular Black Holes in Anti-de Sitter Space

Robie A. Hennigar,[a] **David Kubizňák**,[b] **Sebastian Murk**,[c] **Ioannis Soranidis**[d]

[a] *Centre for Particle Theory, Department of Mathematical Sciences, Durham University, Durham DH1 3LE, UK*

[b] *Institute of Theoretical Physics, Faculty of Mathematics and Physics, Charles University, V Holešovičkách 2, 180 00 Prague 8, Czech Republic*

[c] *Quantum Gravity Unit, Okinawa Institute of Science and Technology, 1919-1 Tancha, Onna-son, Okinawa 904-0495, Japan*

[d] *School of Mathematical and Physical Sciences, Macquarie University, Sydney, New South Wales 2109, Australia*

Additional results included in the paper

1. Regularity with matter: general sufficient conditions when $T^t_t = T^r_r$.
2. Regular black branes $(k=0)$ are generically inner-extremal and have Einstein-like thermodynamics.
3. Regular topological black holes $(k=-1)$: after compactification, $r=0$ is a chronology horizon.
4. Charged spherical black holes: one critical point; the critical ratio depends on charge and coupling.
5. Topological thermodynamics: from no criticality to reverse van der Waals behavior.

JHEP **2025** (11), 121

arXiv:2505.11623 [gr-qc]

Thermodynamics of Regular Black Holes in Anti-de Sitter Space

Robie A. Hennigar[a] **David Kubizňák**[b] **Sebastian Murk**[c] **Ioannis Soranidis**[d]

[a] *Centre for Particle Theory, Department of Mathematical Sciences, Durham University, Durham DH1 3LE, UK*

[b] *Institute of Theoretical Physics, Faculty of Mathematics and Physics, Charles University, V Holešovičkách 2, 180 00 Prague 8, Czech Republic*

[c] *Quantum Gravity Unit, Okinawa Institute of Science and Technology, 1919-1 Tancha, Onna-son, Okinawa 904-0495, Japan*

[d] *School of Mathematical and Physical Sciences, Macquarie University, Sydney, New South Wales 2109, Australia*

Backup slides

Sufficient conditions for curvature regularity

To guarantee a fully regular solution for the full range of $r \in [0, \infty)$, it is sufficient for $h_f(x)$ to be a monotonic function with a divergence, provided that $\mathcal{S}(r)$ and its derivatives have no divergences at finite r.

NB:

1. As these conditions are only sufficient but not necessary, many other resummations with nonsingular black holes will exist.
2. For a given resummation $h_f(x)$, the function $\mathcal{S}(r)$ determines the domain of ψ. Therefore, it is entirely possible for a resummation that is nonsingular in vaccum to become singular when certain matter content is added.

Example: Hayward resummation $h_{\mathrm{f}}(\psi) = \dfrac{\psi}{1 - \alpha\psi}$

Monotonic only on the disjoint intervals $\psi \in (-\infty, 1/\alpha)$ and $\psi \in (1/\alpha, \infty)$

If $\mathcal{S}(r)$ is not of uniform sign, the Hayward model may not be able to accommodate it within a single domain for ψ.

To ensure RBHs exist regardless of the matter content, we must select a resummation $h_f(x)$ with range $(-\infty, \infty)$ in a single domain on which it is a monotonic function

Asymptotic and near-core behavior

Asymptotically flat vacuum ($\boldsymbol{\Lambda = 0, k = +1}$):

$$f(r) = 1 - \frac{m}{r^{D-3}} + \cdots\,, \qquad \text{as } r \to \infty,$$

Asymptotically AdS ($\boldsymbol{\Lambda < 0, k \in \{-1, 0, +1\}}$):

$$f(r) = k + \frac{r^2}{L_{\text{eff}}^2} - \frac{G_{\text{eff}}}{G_N}\frac{m}{r^{D-3}} + \cdots\,, \qquad \text{as } r \to \infty,$$

Near-core behavior ($\boldsymbol{k \in \{-1, 0, +1\}}$):

$$f(r) = k - \frac{r^2}{|\alpha|} + \cdots\,, \qquad \text{as } r \to 0.$$

$$L_{\text{eff}}^2 = -\frac{1}{h_{\text{f}}^{-1}\left(-1/L^2\right)},$$

$$G_{\text{eff}} = \frac{G_{\text{N}}}{h_{\text{f}}'\left(-1/L_{\text{eff}}^2\right)}.$$

Critical mass parameter $(\Lambda = 0, k = +1)$

For all 7 models in Table 1, there exists a critical value of the mass m_{cr} which demarcates the possible solutions.

1. For $m > m_{\mathrm{cr}}$, there is an event and inner horizon.
2. For $m = m_{\mathrm{cr}}$, there is a single degenerate horizon representing an extremal black hole with vanishing Hawking temperature.
3. For $0 < m < m_{\mathrm{cr}}$, there are no horizons. These represent gravitational solitons: Lorentzian, finite energy, geodesically complete metrics.

Example: Hayward resummation

$$m_{\mathrm{cr}} = \frac{(D-1)^{(D-1)/2}}{2(D-3)^{(D-3)/2}}\alpha^{(D-3)/2}$$

Explicit expressions for thermodynamic potentials

For $k = \pm 1$, the thermodynamic potentials read:

$$M = \frac{(D-2)\Omega_{D-2} r_+^{D-1}}{16\pi G_\mathrm{N}} h(\psi_+) + \frac{(D-2)\Omega_{D-2}}{16\pi G_\mathrm{N}} \frac{r_+^{D-1}}{L^2} + \Omega_{D-2} \int_\infty^{r_+} r^{D-2} T_t^t \mathrm{d}r \,,$$

$$T = -\frac{1}{4\pi r_+} \left[\frac{r_+^3 \mathcal{S}'(r_+)}{h'(\psi_+)} + 2k \right] , \quad S = \frac{(D-2)\Omega_{D-2}}{4G_\mathrm{N}} \int r_+^{D-3} h_\mathrm{f}'(k/r_+^2) \mathrm{d}r_+ \,,$$

$$V = \frac{\Omega_{D-2} r_+^{D-1}}{D-1} , \qquad P = -\frac{\Lambda}{8\pi G_\mathrm{N}} = \frac{(D-1)(D-2)}{16\pi G_\mathrm{N} L^2} ,$$

$$\Psi = \frac{1}{2\alpha} \left[(D-3)M - (D-2)TS + 2PV \right] .$$

Table 1: Summary of models

Model	α_n	$h_{\mathrm{f}}(\psi)$	$f(r)$
I	α^{n-1}	$\dfrac{\psi}{1-\alpha\psi}$	$k-\dfrac{r^2\mathcal{S}(r)}{1+\alpha\mathcal{S}(r)}$
II	$\dfrac{\alpha^{n-1}}{n}$	$-\dfrac{\log(1-\alpha\psi)}{\alpha}$	$k-\dfrac{r^2}{\alpha}\left(1-e^{-\alpha\mathcal{S}(r)}\right)$
III	$n\alpha^{n-1}$	$\dfrac{\psi}{(1-\alpha\psi)^2}$	$k-\dfrac{r^2\left[1+2\alpha\mathcal{S}(r)-\sqrt{1+4\alpha\mathcal{S}(r)}\right]}{2\alpha^2\mathcal{S}(r)}$
IV	$\dfrac{(1-(-1)^n)}{2}\alpha^{n-1}$	$\dfrac{\psi}{1-\alpha^2\psi^2}$	$k+\dfrac{r^2\left[1-\sqrt{1+4\alpha^2\mathcal{S}^2(r)}\right]}{2\alpha^2\mathcal{S}(r)}$
V	$\dfrac{(1-(-1)^n)\Gamma\left(\frac{n}{2}\right)}{2\sqrt{\pi}\Gamma\left(\frac{n+1}{2}\right)}\alpha^{n-1}$	$\dfrac{\psi}{\sqrt{1-\alpha^2\psi^2}}$	$k-\dfrac{r^2\mathcal{S}(r)}{\sqrt{1+\alpha^2\mathcal{S}^2(r)}}$
VI	$\dfrac{\left(1+(-1)^{(n+1)}\right)}{2n}\alpha^{n-1}$	$\dfrac{\operatorname{arctanh}(\alpha\psi)}{\alpha}$	$k-\dfrac{r^2}{\alpha}\tanh\left(\alpha\mathcal{S}(r)\right)$
VII	N/A	$\dfrac{\psi}{(1-\alpha^{\mathrm{N}}\psi^{\mathrm{N}})^{1/\mathrm{N}}}$	$k-\dfrac{r^2\mathcal{S}(r)}{\left[1+\alpha^{\mathrm{N}}\mathcal{S}^{\mathrm{N}}(r)\right]^{1/\mathrm{N}}}$

Table 1. Models: summary. Example resummations and their corresponding exact solutions to the equations of motion. Here, we write the metric function for general minimally coupled matter satisfying $T_t^t = T_r^r$ in terms of the function $\mathcal{S}(r)$ introduced in eq. (2.16). In the case of Model VII, the coefficients of the series can be obtained by expanding $h_{\mathrm{f}}(\psi)$ for a given value of N (a closed form expression is not simple for general N). Note that this model includes Models I and V as special cases. Models I, II, and III are valid only in odd dimensions. Models IV, V and VI are valid in odd dimensions and also for $D = 4(k+1)$ with $k \in \mathbb{Z}^+$. Model VII is valid in odd dimensions for general N, while particular cases of N also yield resummations valid in even dimensions. The simplest case for an even dimension D is given by $\mathrm{N} = D/2$.

Table 2: Effective couplings and parameter constraints

Model	$h(\psi)$	L_{eff}^2/L^2	$G_{\text{eff}}/G_{\text{N}}$	Parameter constraints
I	$\frac{\psi}{1-\alpha\psi}$	$1-a$	$\frac{1}{(1-a)^2}$	$0<a<1$
II	$-\frac{\log(1-\alpha\psi)}{\alpha}$	$\frac{a}{e^a-1}$	e^a	$a>0$
III	$\frac{\psi}{(1-\alpha\psi)^2}$	$\frac{2a^2}{1-2a-\sqrt{1-4a}}$	$\frac{2-8a+2\sqrt{1-4a}(-1+2a)}{4a^2(-1+4a)}$	$0<a<\frac{1}{4}$
IV	$\frac{\psi}{1-\alpha^2\psi^2}$	$\frac{2a^2}{-1+\sqrt{1+4a^2}}$	$\frac{1}{2a^2}\left[1-\frac{1}{\sqrt{1+4a^2}}\right]$	$a\in\mathbb{R}$
V	$\frac{\psi}{\sqrt{1-\alpha^2\psi^2}}$	$\sqrt{1+a^2}$	$\left(1+a^2\right)^{-3/2}$	$a\in\mathbb{R}$
VI	$\frac{\text{arctanh}(\alpha\psi)}{\alpha}$	$a\coth a$	$\text{sech}^2\, a$	$a>0$
VII	$\frac{\psi}{(1-\alpha^{\text{N}}\psi^{\text{N}})^{1/\text{N}}}$	$\left[1+(-a)^{\text{N}}\right]^{1/\text{N}}$	$\left[1+(-a)^{\text{N}}\right]^{-\frac{(\text{N}+1)}{\text{N}}}$	$\begin{cases} a\in\mathbb{R} & \text{if N even} \\ 0<a<1 & \text{if N odd}\end{cases}$

Table 2. Models: effective couplings and parameter constraints. We tabulate the effective AdS length L_{eff} and the effective Newton constant G_{eff} for each of the resummations that appear in table 1. We have defined $a=\alpha/L^2$ to ease the notation. The final column of the table gives the range of a for which the metrics are fully regular and have AdS asymptotics.

Table 3: Infinite-dimensional limit of critical ratio

Model	I	II	III	IV	V	VI
$h(\psi)$	$\dfrac{\psi}{1-\alpha\psi}$	$-\dfrac{\log(1-\alpha\psi)}{\alpha}$	$\dfrac{\psi}{(1-\alpha\psi)^2}$	$\dfrac{\psi}{1-\alpha^2\psi^2}$	$\dfrac{\psi}{\sqrt{1-\alpha^2\psi^2}}$	$\dfrac{\mathrm{arctanh}(\alpha\psi)}{\alpha}$
$\lim\limits_{D\to\infty}\dfrac{P_c v_c}{T_c}$	$\dfrac{3}{8}=0.375$	0.386193	0.362512	0.402311	0.406247	0.408348

Table 3. Ultimate critical ratio: limit of infinite dimensions. We tabulate the critical ratios for the vacuum-AdS regular black holes for the different models in the strict $D \to \infty$ limit. The result for model I is exact, and independent of dimension. All other models exhibit weak dependence on dimension, and the $D \to \infty$ value provides a good approximation for general dimensions. Despite the very different functional forms for the different models, the critical ratios of all models fall within ≈ 0.04 of each other.

Table 4: NEC and SEC

	$q = 0$		$q \neq 0$	
	NEC	SEC	NEC	SEC
Model I	✓(✓)	✗(✗)	✗(✗)	✗(✓)
Model IV	✗(✓)	✗(✗)	✗(✗)	✗(✓)
Model V	✗(✓)	✗(✗)	✗(✗)	✗(✓)

Table 4. NEC and SEC: summary. Status of the NEC and SEC for the cosmological extensions of models I (Hayward), IV, and V of table 1 with and without charge. The behavior near the center is indicated in parentheses.

Figure 1: Horizon structure of spherical AdS solutions

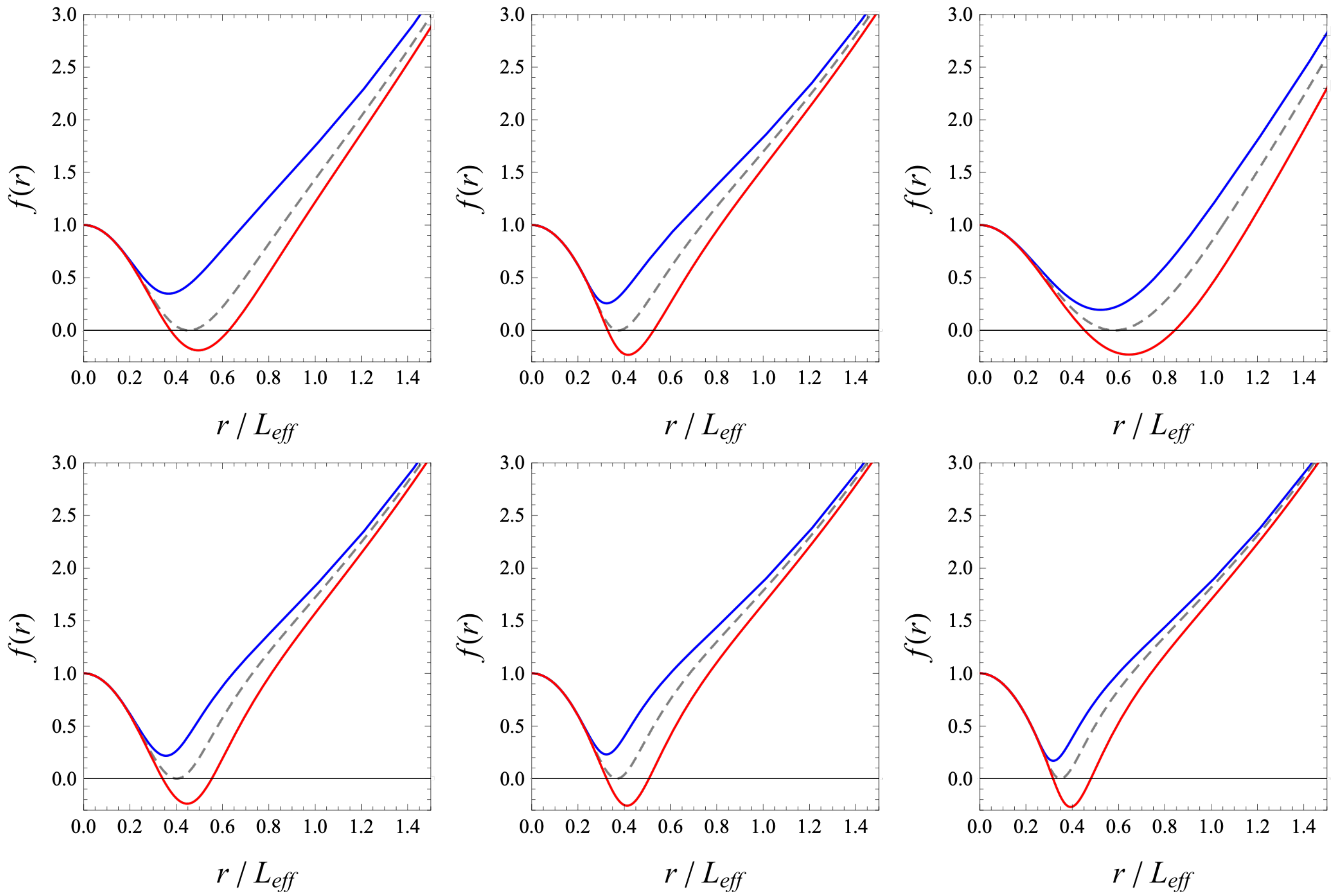

Figure 1. Metric functions: AdS black holes. Plots of the $k = 1$ metric function for models I–VI for different values of the thermodynamic mass M. In each plot we have set $L_{\text{eff}} = 1$, $G_{\text{eff}} = 1$, $a = 0.1$, and $D = 5$. The top row represents models I–III from left to right, while the bottom row corresponds to models IV–VI in the same order. The gray dashed line represents the critical thermodynamic mass value associated with an extremal regular black hole. The values of the thermodynamic mass M in the color order [blue, gray, red] are: $[0.3, 0.706, 1]$ (top left), $[0.2, 0.362, 0.55]$ (top center), $[1.2, 1.849, 2.8]$ (top right), $[0.2, 0.326, 0.5]$ (bottom left), $[0.15, 0.253, 0.4]$ (bottom center), and $[0.15, 0.217, 0.35]$ (bottom right). All models I–VI yield metric functions that have exactly the same qualitative structure.

Figure 2: Metric functions of Maxwell charged BHs

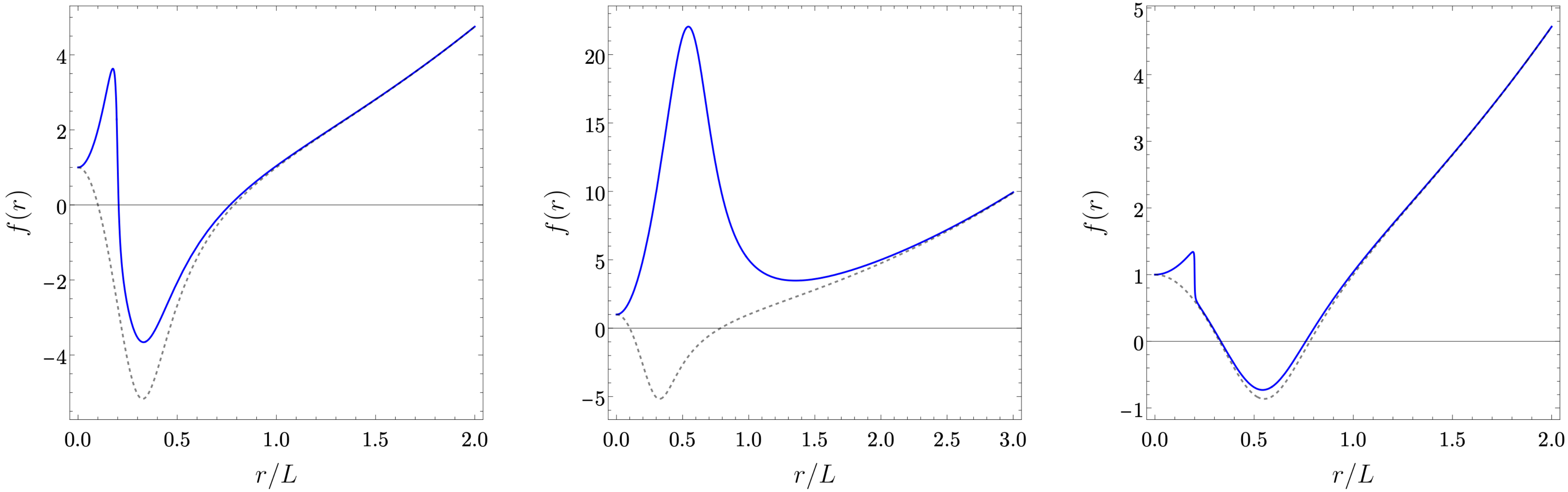

Figure 2. Metric functions: Maxwell charged black holes. Plots of the $k = +1$ metric function for model IV for different values of the coupling and charge. In each plot, we have set $L = 1$, $m = 1$, and $D = 5$. We have also included the corresponding metric function with $q = 0$, shown in each panel as the dashed gray curve. The parameter values are: $\alpha = 1/100, q = 1/20$ (left), $\alpha = 1/100, q = 2$ (center) and $\alpha = 1/10, q = 1/20$ (right). Models V, VI and VII with N even yield metric functions that have exactly the same qualitative structure.

Figure 3: Metric functions of black branes

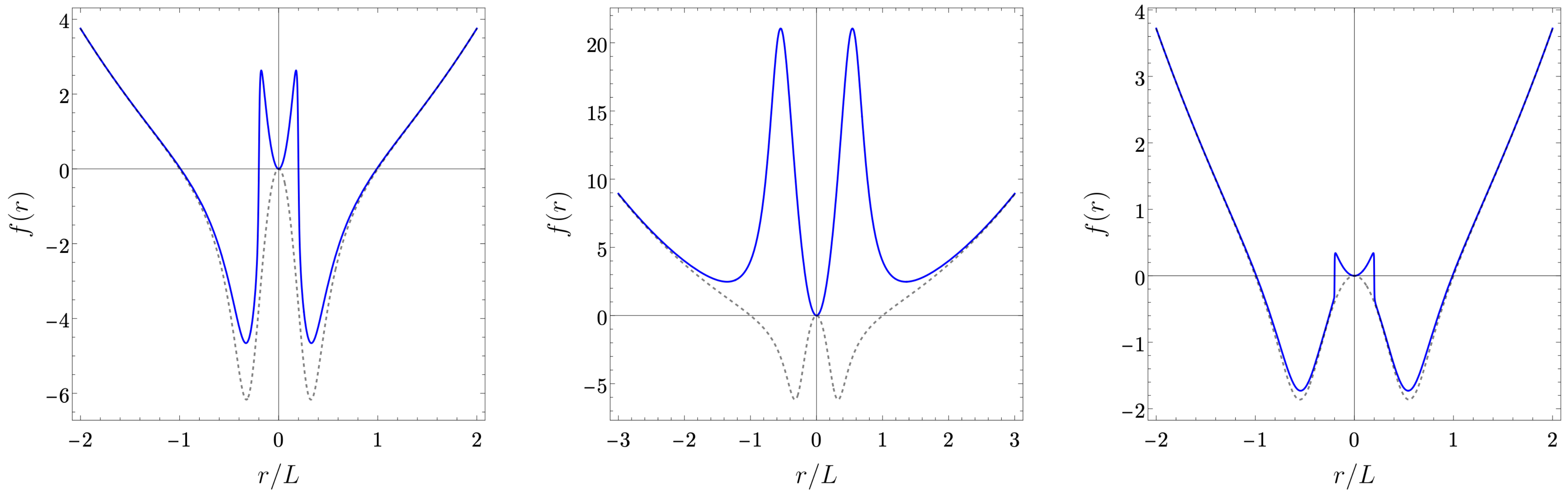

Figure 3. Metric functions: black branes. Plots of the $k = 0$ metric function for model IV for different values of the coupling and charge. In each plot, we have set $L = 1$, $m = 1$, and $D = 5$. We have also included the corresponding metric function with $q = 0$, shown in each panel as the dashed gray curve. The parameter values are: $\alpha = 1/100, q = 1/20$ (left), $\alpha = 1/100, q = 2$ (center) and $\alpha = 1/10, q = 1/20$ (right). Models V, VI and VII with N even yield metric functions that have exactly the same qualitative structure.

Figure 4: Metric functions of charged BHs in NLE

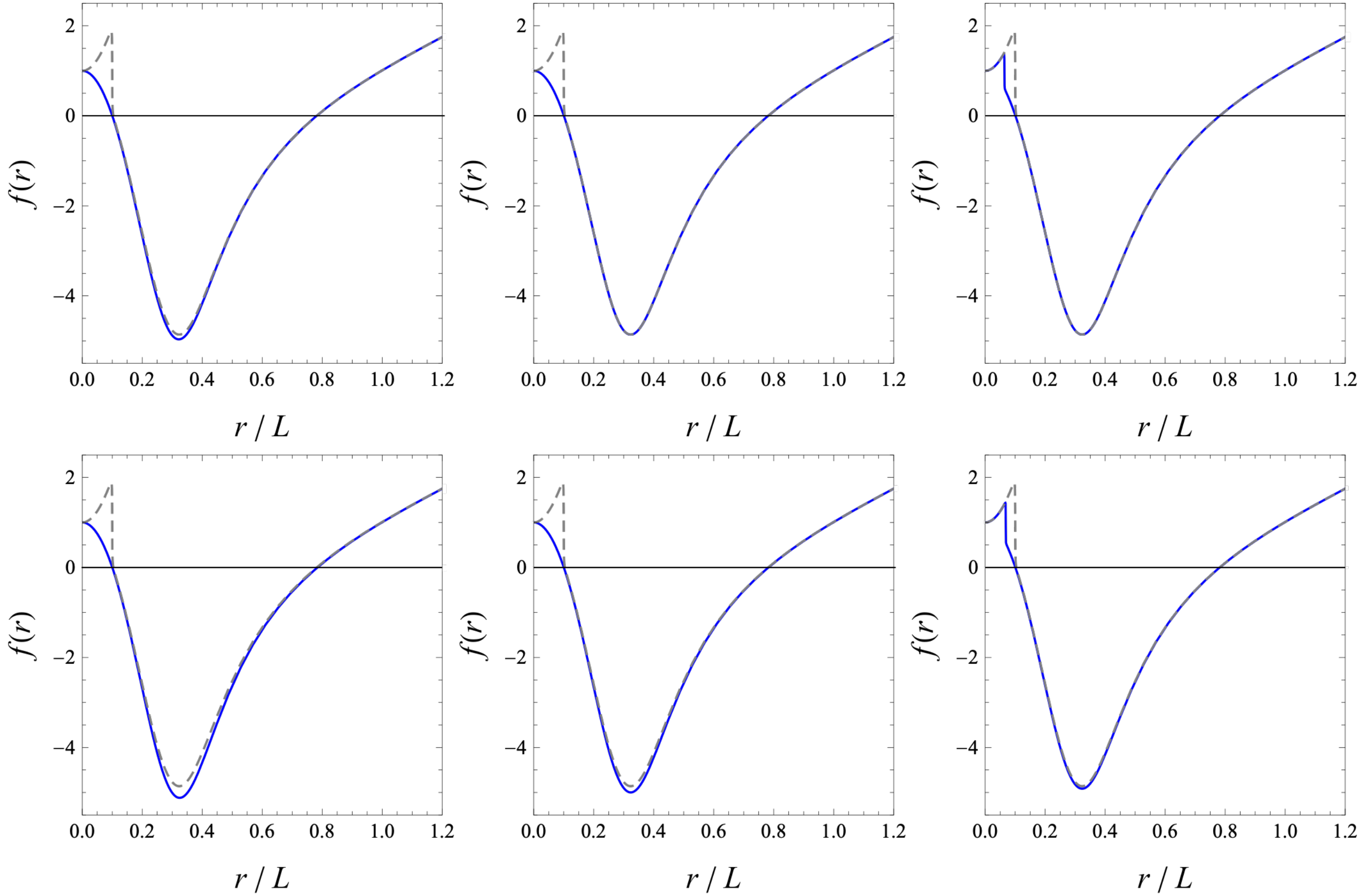

Figure 4. Metric functions: charged black holes in nonlinear electrodynamics. Plots of the $k = 1$ metric function for model IV, where we have set $m = 1$, $L = 1$, $\alpha = 0.01$, $q = 0.1$, and $D = 5$ for two different NLE Lagrangians illustrated by the blue solid line. The Maxwell case is shown as a gray dashed line. **Top:** Born — Infeld case for $m > m_\star$ (left), $m = m_\star$ (middle), and $m < m_\star$ (right), achieved by choosing $b = 1$, $b \simeq 20.07$, and $b = 40$, respectively; **Bottom:** RegMax case for $m > m_\star$ (left), $m = m_\star$ (middle), and $m < m_\star$ (right), achieved by choosing $\beta = 1$, $\beta \simeq 4.46$, and $\beta = 15$, respectively. Both Born-Infeld and RegMax metric functions have exactly the same qualitative structure.

Figure 5: Wald entropy of Hayward AdS model

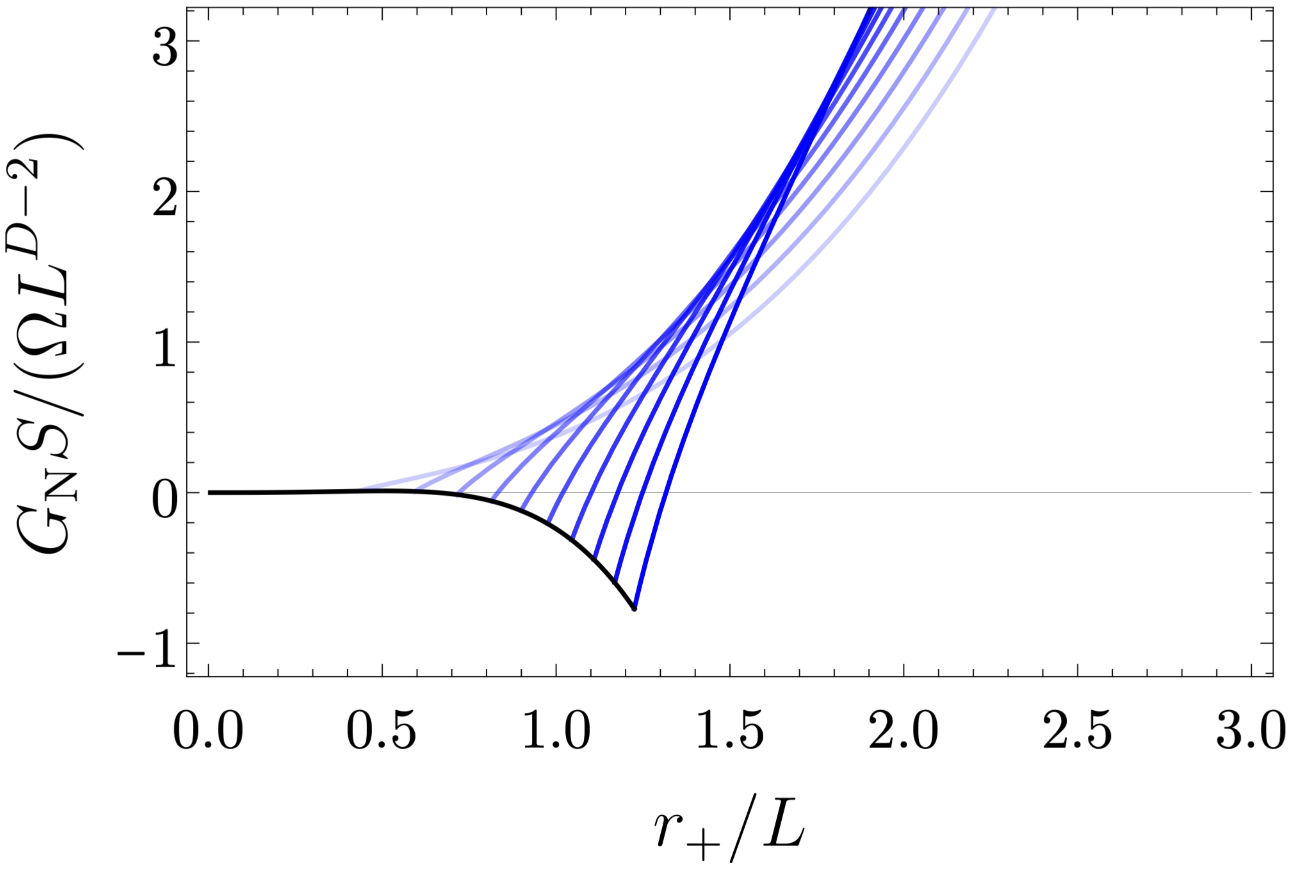

Figure 5. Wald entropy: Hayward-AdS model. The Wald entropy is plotted as a function of the horizon radius for the Hayward model in $D = 5$. The blue curves show the entropy for different values of $a = \alpha/L^2$, ranging from $a = 0$ to the maximum allowed value of $a = 1$ from the lightest to the darkest hue. The black curve shows the entropy at extremality, with all blue curves originating along this line. Plots in higher dimensions are qualitatively similar.

Figure 6: P-v diagram of Hayward AdS model

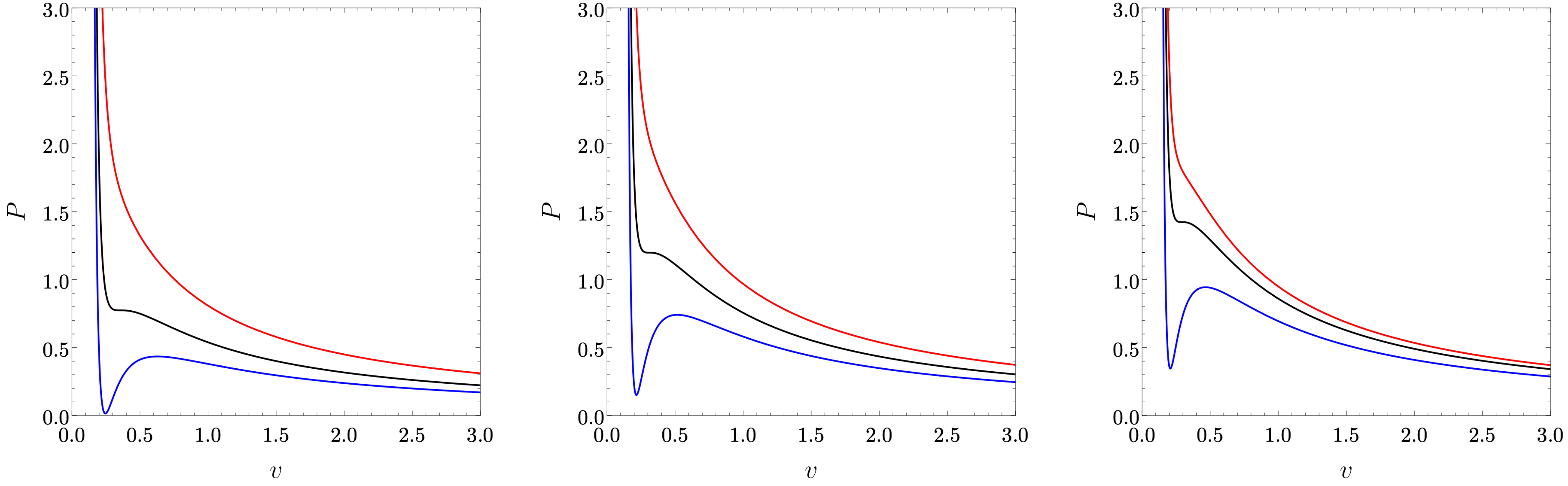

Figure 6. $P - v$ diagram: Hayward-AdS black hole. Isotherms for the Hayward-AdS black hole (model I) for $D = 5, 7, 9$ (from left to right). In each case, the lower blue curve has $T < T_c$, the middle black curve has $T = T_c$, and the upper red curve has $T > T_c$. In each plot, we have set the effective molecular size parameter $b = 0.1$. The units are such that $G_\mathrm{N} = 1$.

Figure 7: Free energy of Hayward AdS model

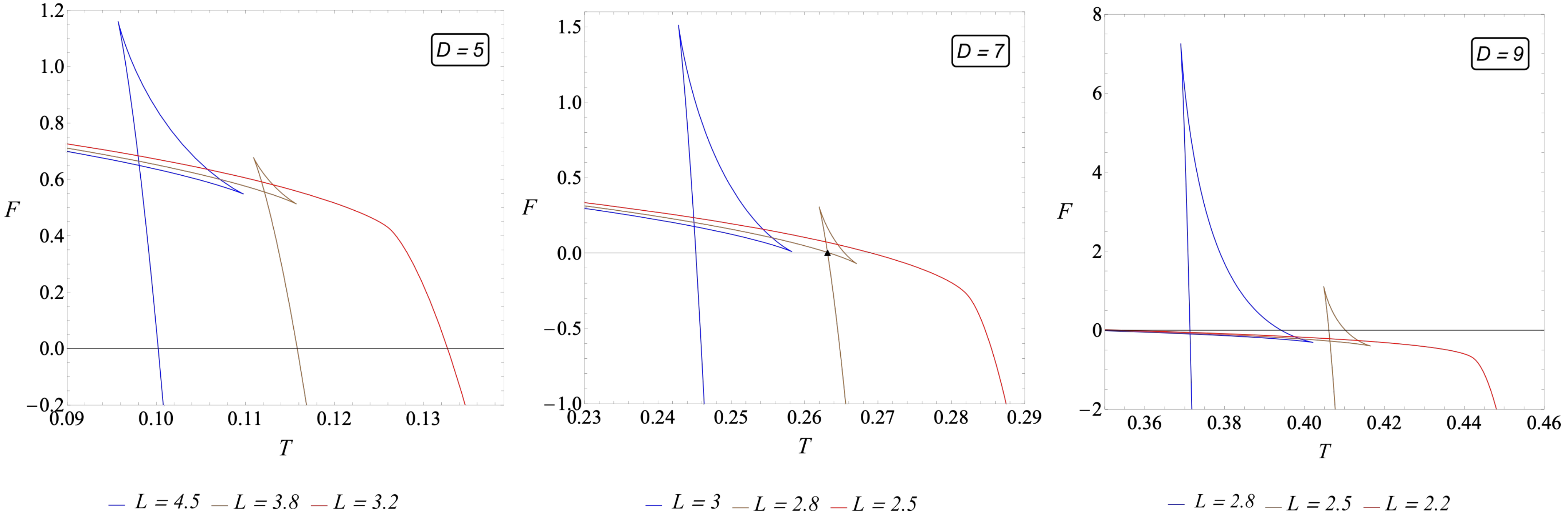

Figure 7. Free energy: Hayward-AdS model. The free energy F is plotted parametrically as a function of temperature T, using the horizon radius as a parameter, for the Hayward-AdS black hole (model I) in various dimensions. The coupling α remains fixed at the value $\alpha = 0.2$, and we allow the cosmological constant parameter L to vary. In the $D = 7$ case, the triangle indicates the triple point where the small black hole, large black hole, and radiation phases coexist (see also figure 8). The temperature range was chosen to zoom in on the regions with interesting behavior. The units are such that $G_{\mathrm{N}} = 1$.

Figure 8: Phase diagram of Hayward AdS model

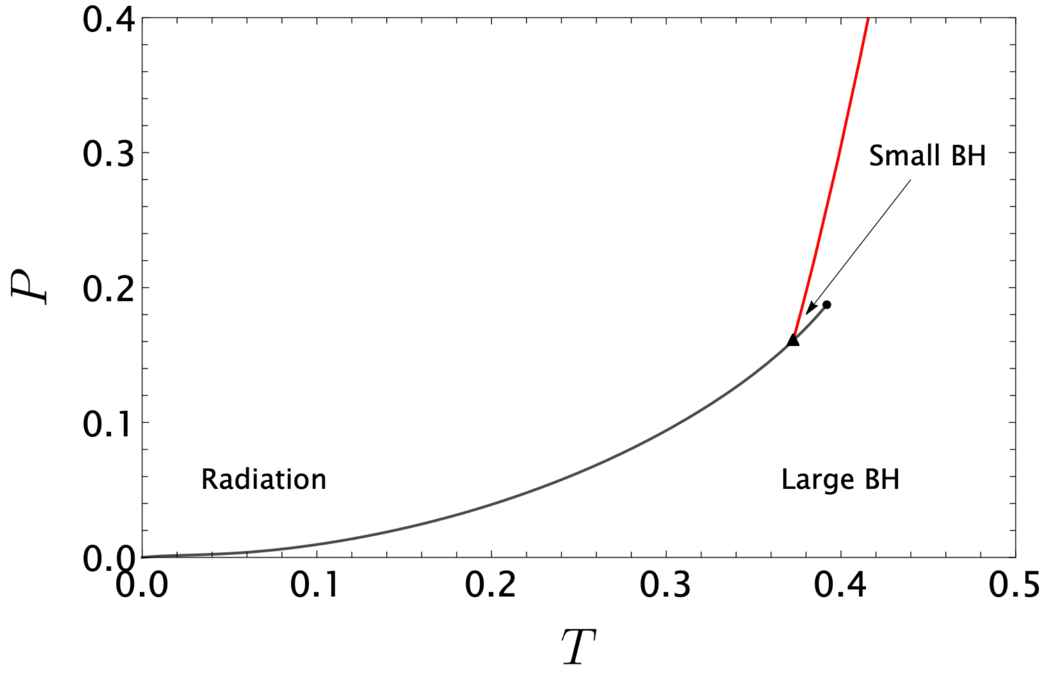

Figure 8. Phase diagram: Hayward-AdS model. The pressure P is plotted as a function of temperature T for the $D = 7$ case with a fixed coupling parameter $\alpha = 0.1$. The coexistence lines separate regions corresponding to the small black hole, large black hole, and radiation phases. As the temperature increases from low values, the black line follows the coexistence between the radiation and large black hole phases, ending at the triangle, which marks the triple point where all three phases coexist. Beyond this point, the black line represents the coexistence of small and large black hole phases, ending at the dot that denotes the critical point. The red line represents the coexistence between the radiation and large black hole phases at pressures above the triple point, ending at the maximum pressure $P_{\rm max} = (D-1)(D-2)/(16\pi G_{\rm N}\alpha)$, imposed by the condition $L^2 > \alpha$. For the chosen value of α, this corresponds to $P_{\rm max} \approx 5.97$. This point is not visible in the figure, as the plot is zoomed in on the region where the most interesting features of the phase diagram appear. The units are such that $G_{\rm N} = 1$.

Figure 9: Critical ratio of various AdS models

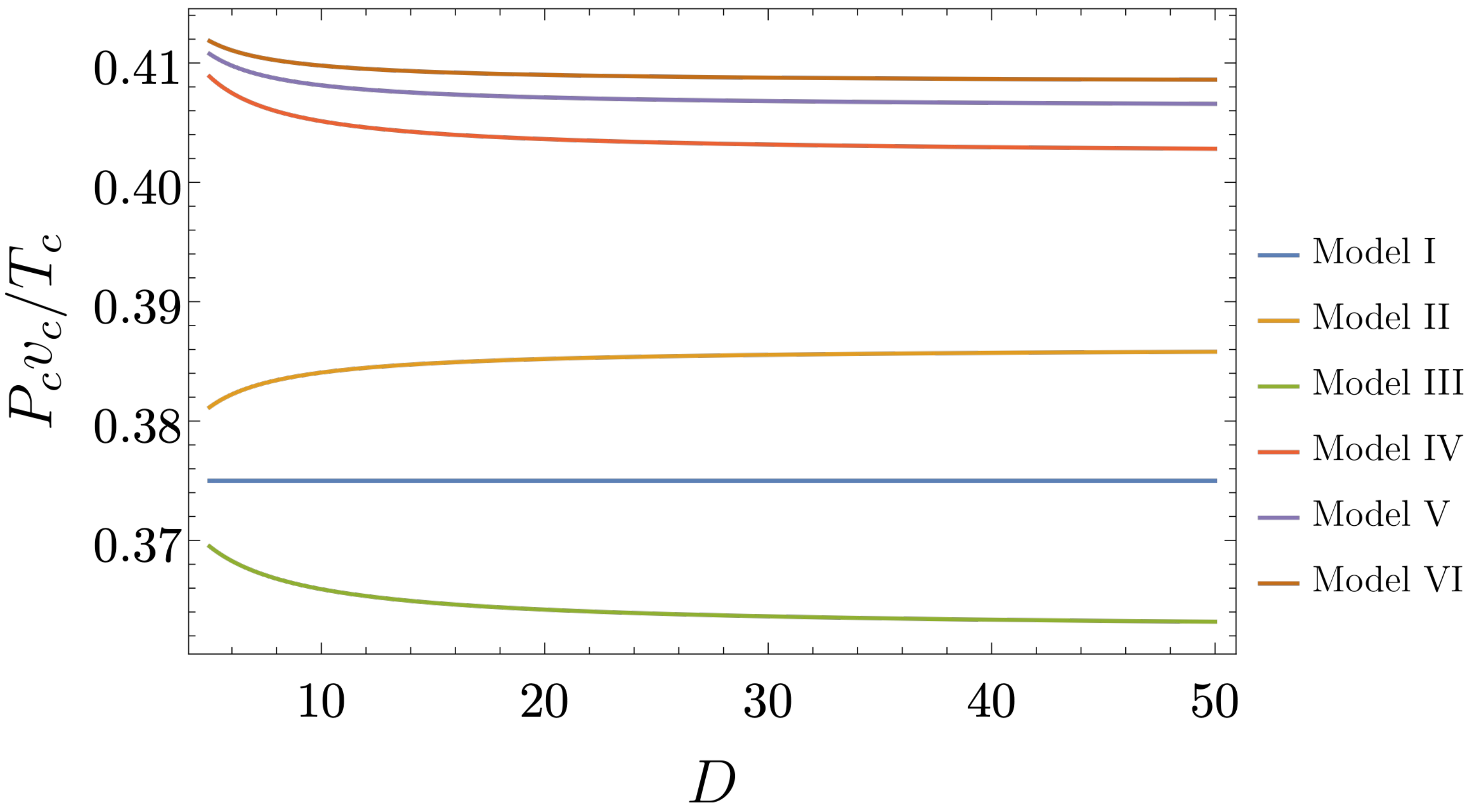

Figure 9. Critical ratio $P_c v_c/T_c$: various AdS models. We display a dimensional dependence of the critical ratio for the first six models in table 1 in vacuum-AdS. The Hayward-AdS case (model I) is the unique one for which the critical ratio matches that of the van der Waals fluid, and is also the unique one for which the critical ratio is independent of dimension. The plot illustrates that, while the other models exhibit dimensional dependence, it is very weak. Note that we have interpolated between integer dimensions.

Figure 10: Charge dependence of critical ratio

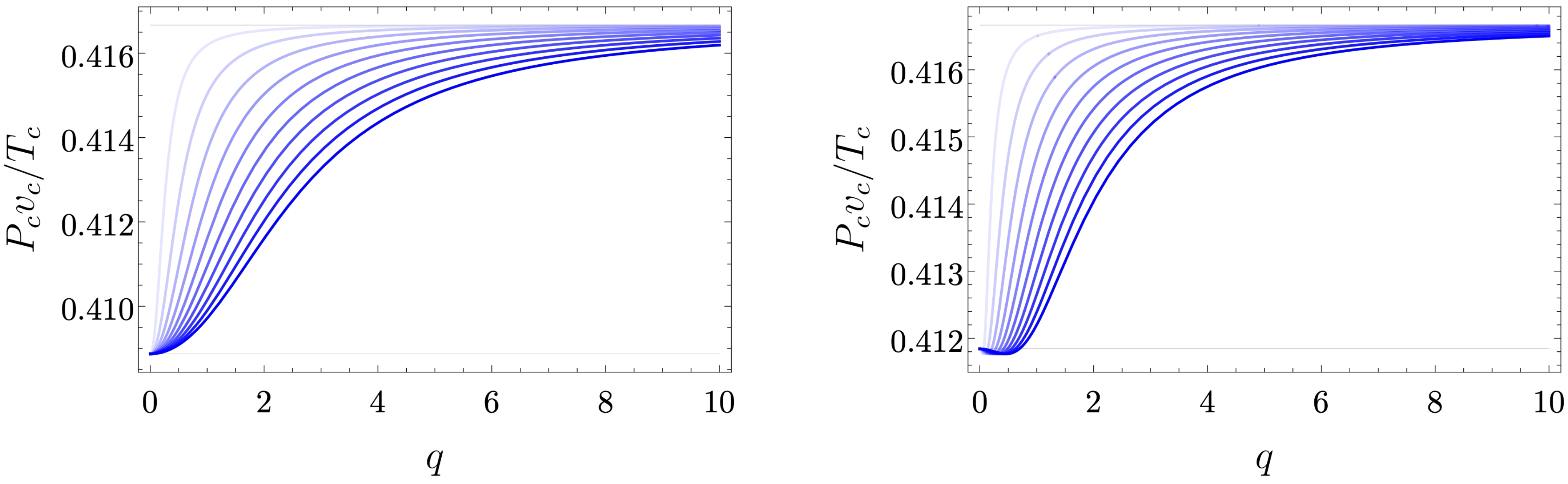

Figure 10. Critical ratio: charge dependence. Ratio of critical parameters for Maxwell charged black holes in model IV (left) and model VI (right) in the five-dimensional case. The blue curves correspond to different values of α, with the lighter (upper-leftmost) curves corresponding to smaller values, and the darker curves corresponding to larger values. The lower horizontal line is the $q = 0$ critical ratio, while the upper horizontal line is the critical ratio in the Einstein-Maxwell theory. The units are such that $G_{\mathrm{N}} = 1$.

Figure 11: Free energy in the charged Maxwell case

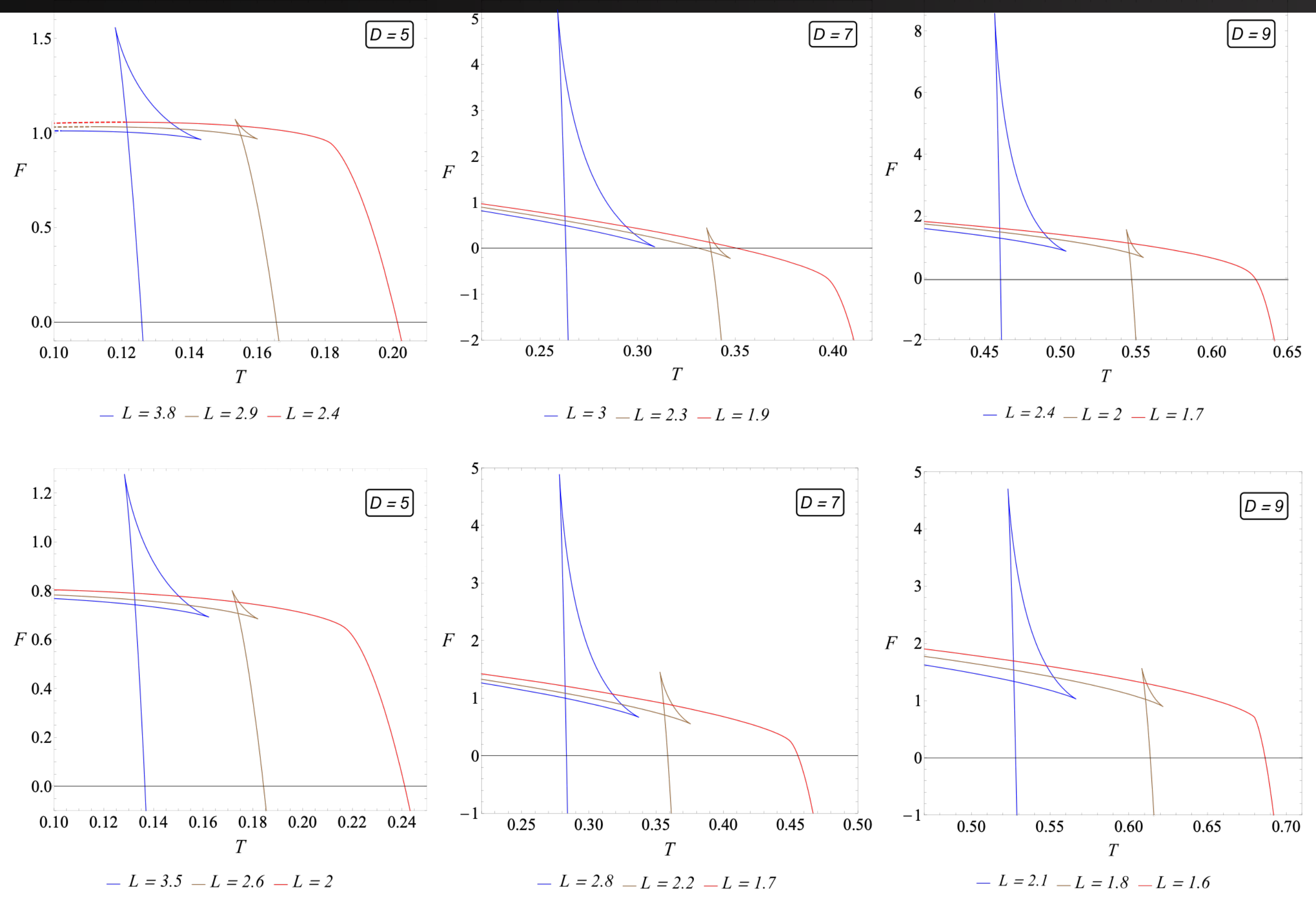

Figure 11. Free energy: charged Maxwell case. The free energy F is plotted parametrically as a function of temperature T, using the horizon radius as a parameter, for model IV (top) and model VI (bottom), both minimally coupled to the Maxwell field, across various dimensions. The coupling α and charge parameter q remain fixed at the values $\alpha = 0.2$ and $q = 0.3$, respectively, and we allow the cosmological constant parameter L to vary. The dashed lines indicate branches of black holes with negative Wald entropy. However, in the plots above these are only visible for $D = 5$ in the top left as the temperature range has been chosen to zoom in on the regions with interesting behavior. The units are such that $G_{\rm N} = 1$.

Figure 12: Free energy in Born-Infeld vs. RegMax NLE

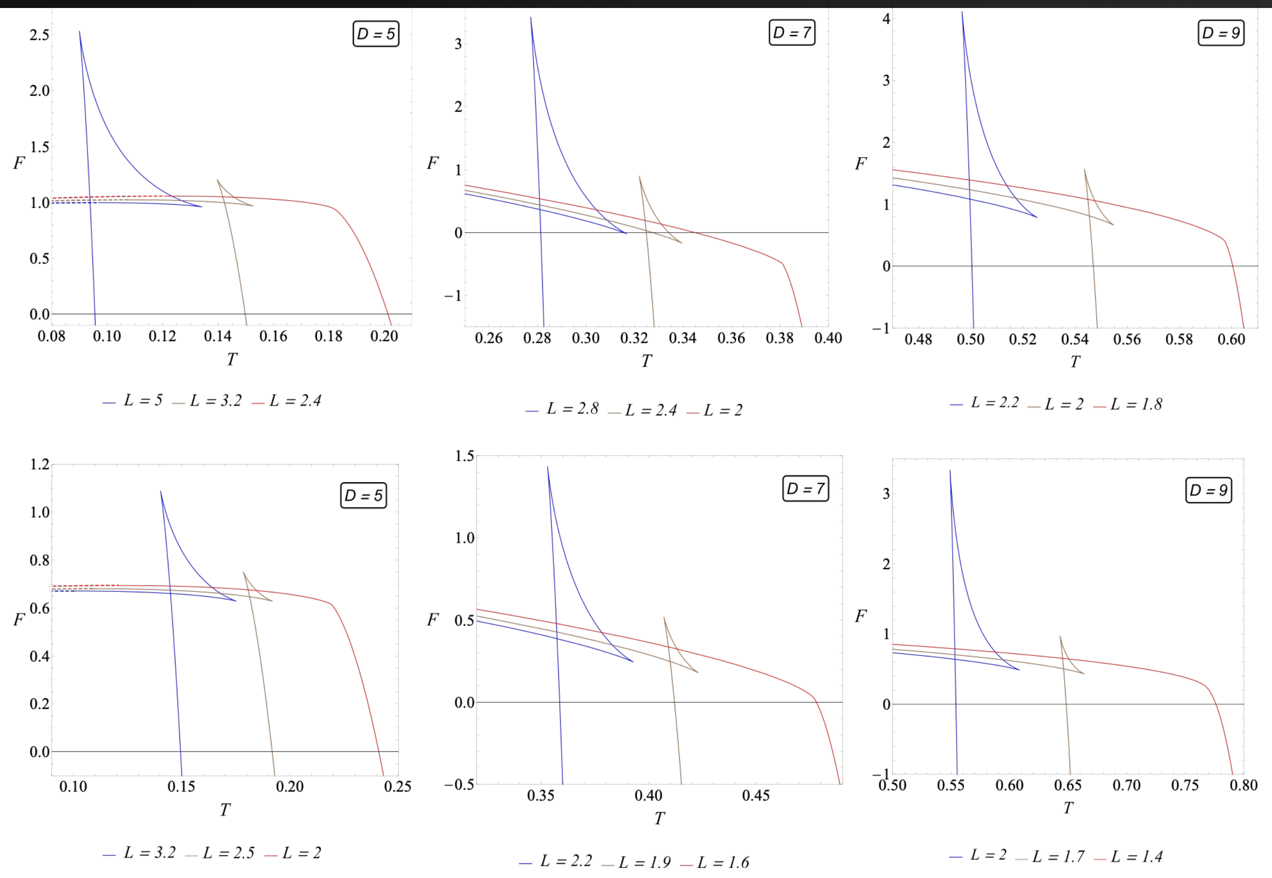

Figure 12. Free energy: Born-Infeld and RegMax cases. The free energy F is plotted parametrically as a function of temperature T, using the horizon radius as a parameter across various dimensions. The coupling α and charge parameter q remain fixed at the values $\alpha = 0.2$ and $q = 0.3$, respectively, and we allow the cosmological constant parameter L to vary. **Top:** model IV, minimally coupled to the Born-Infeld field, with the electric field regularization parameter fixed at $b = 10$. **Bottom:** model VI, minimally coupled to the RegMax field, with the electric field regularization parameter fixed at $\beta = 4$. The dashed lines indicate branches of black holes with negative Wald entropy. However, in the plots above these are only visible for $D = 5$ (left column) as the temperature range has been chosen to zoom in on regions displaying interesting behavior. The units are such that $G_{\mathrm{N}} = 1$.

Figure 13: Free energy for topological BHs

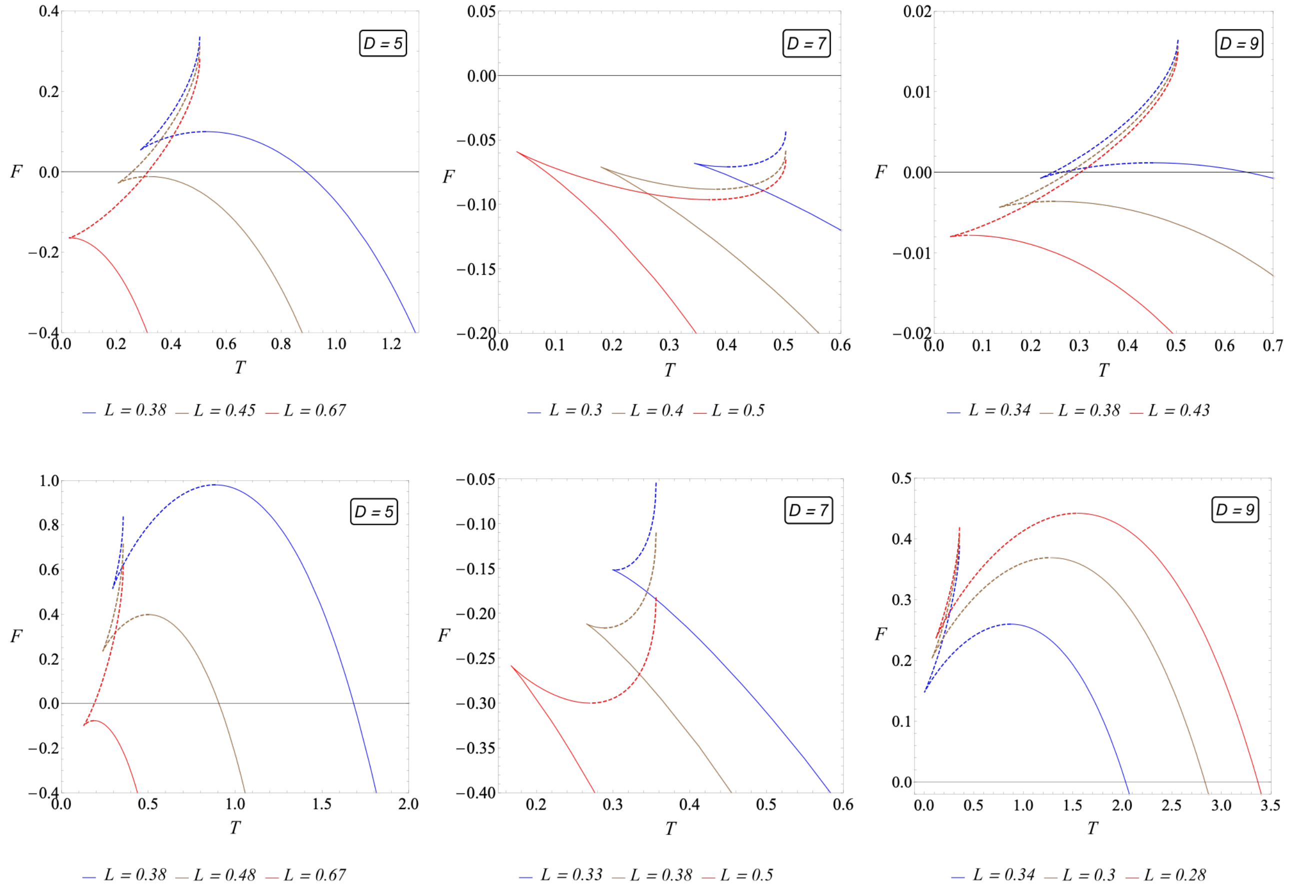

Figure 13. Free energy: topological black holes with $\alpha \to -\alpha$ symmetry. The free energy F is plotted parametrically as a function of temperature T, using the horizon radius as a parameter, across various dimensions for the topological black holes with $k = -1$ of model V. **Top:** no matter fields are present, and the coupling is fixed at $\alpha = 0.1$. **Bottom:** Maxwell-charged case with coupling $\alpha = 0.2$ and charge parameter $q = 0.02$. The temperature range has been chosen to zoom in on regions displaying interesting behavior. In all cases, a dashed line indicates a branch of black holes with negative Wald entropy. Note that in all cases the upper branch (which corresponds to negative mass and entropy) is thermally unstable, as indicated by the upward-curving free energy curves. The units are such that $G_{\rm N} = 1$.

Figure 14: P-v diagram for topological Hayward-AdS BH

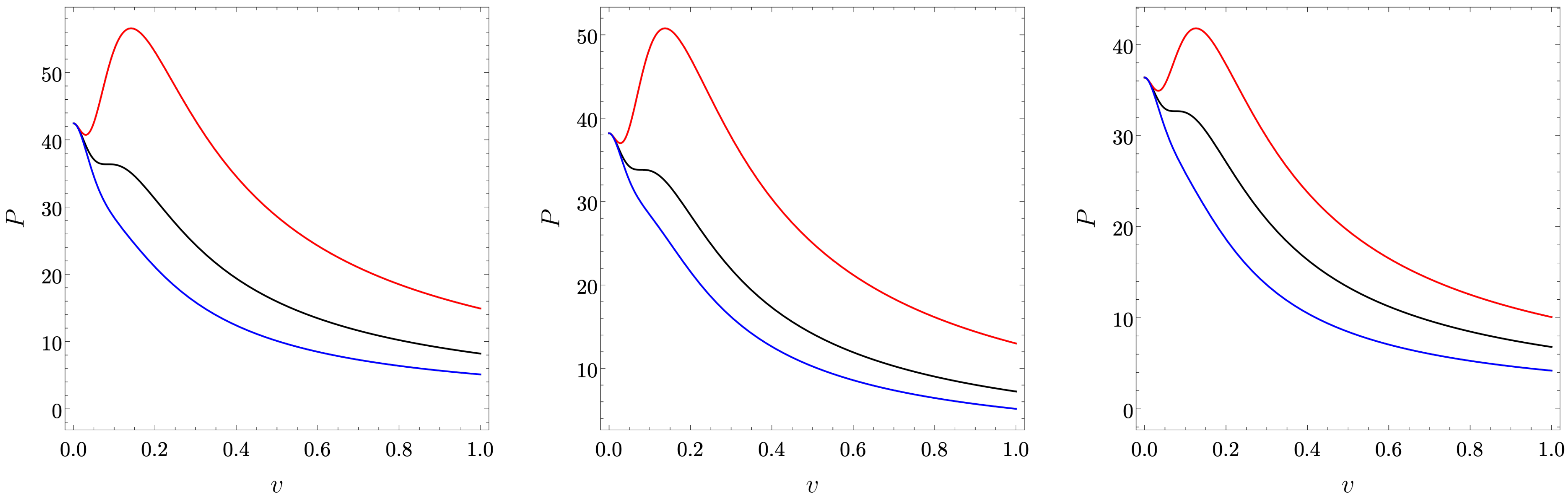

Figure 14. $P - v$ diagram: topological Hayward-AdS black hole. Isotherms for the $k = -1$ Hayward-AdS black hole (model I) for $D = 5, 7, 9$ (left to right) feature a 'reverse van der Waals' behavior. In each case, the lower blue curve has $T < T_c$, the middle black curve has $T = T_c$, and the upper red curve has $T > T_c$. In each plot, we have set the effective molecular size parameter $b = 0.1$. The units are such that $G_{\mathrm{N}} = 1$.

Figure 15: Charge dependence of critical ratio for topological BHs

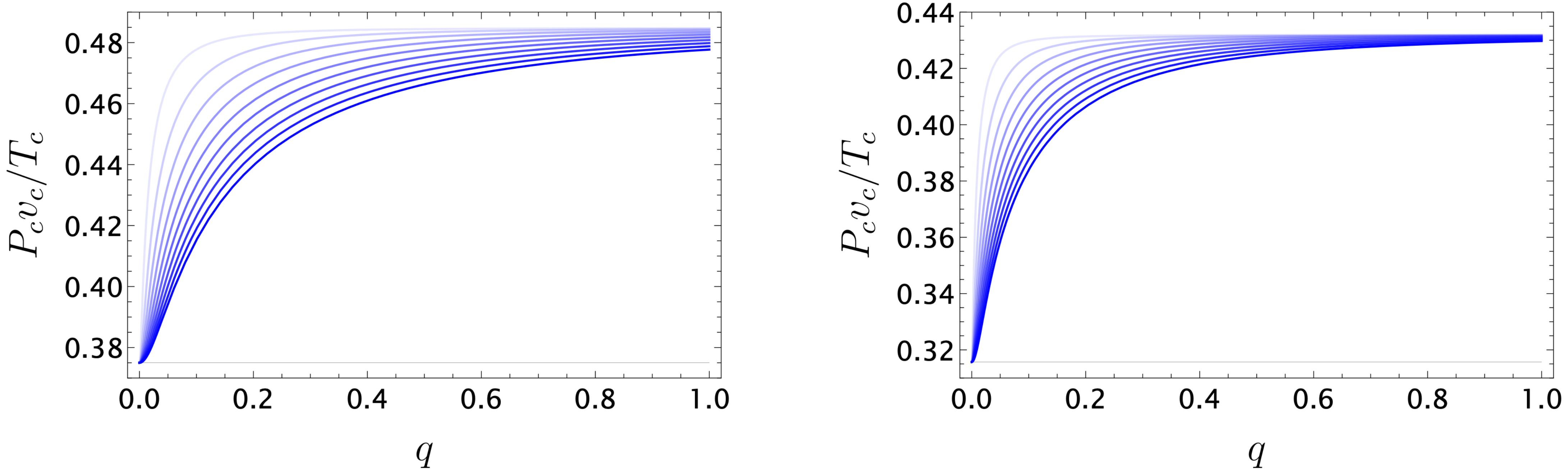

Figure 15. Critical ratio for topological black holes: charge dependence. Ratio of critical parameters for Maxwell charged topological black holes in model I (left) and model II (right) in the five-dimensional case. The blue curves correspond to different values of α, with the lighter (upper-leftmost) curves corresponding to smaller values, and the darker curves corresponding to larger values. The lower horizontal line is the uncharged critical ratio. The units are such that $G_{\mathrm{N}} = 1$.